NTIA-REPORT-78-5

Measuring Characteristics of Microwave Mobile Channels

R. W. Hubbard
R. F. Linfield
W. J. Hartman

U.S. DEPARTMENT OF COMMERCE
Juanita M. Kreps, Secretary

Henry Geller, Assistant Secretary-Designate
for Communications and Information

June 1978

TABLE OF CONTENTS

LIST OF FIGURES

LIST OF TABLES

MEASURING CHARACTERISTICS OF MICROWAVE MOBILE CHANNELS

R.W. Hubbard
R.F. Linfield
W.J. Hartman*

This report describes the application of a high resolution (6 ns) pseudo-random noise (PN) channel probe for evaluating the transmission character of a land-mobile communication channel. Preliminary measurements were performed at a microwave frequency in a number of locations in Boulder, Colorado. Examples of data are presented which characterize the frequency correlation of the channel transfer function, and provide additional information on the spectral distortions caused by multipath.

The data processing and analysis techniques are emphasized in the report, as they are ideally suited to developing a useful statistical summary of channel parameters. The methods are rapid, and are made from data recorded in standard analog magnetic tape in the field locations. It is recommended that a wideband channel characterization program be undertaken in the near future before spectrum congestion precludes obtaining useful data.

Key words: channel characterization; frequency correlation function; impulse response; land-mobile radio; microwaves; multipath

1. INTRODUCTION

There is considerable interest in transmitting digital data including digitized voice signals over mobile links and military tactical nets operating in urban and suburban areas at microwave frequencies. Transmission channels in this operating environment are very lossy and dispersive, both in time and frequency. System performance is limited because many signal components are received

*The authors are with the Institute for Telecommunication Sciences, National Telecommunications and Information Administration, U. S. Department of Commerce, Boulder, CO 80303.

after propagating over different path lengths due to reflections, and the signal amplitude and delay varies with time due to vehicle motion.

Performance of radio systems using these channels may be improved by incorporating adaptive equalization circuitry in the system design. Such techniques not only combat the multipath, but can indeed utilize the inherent diversity of the multipath structure to enhance the grade of service. Consequently, it is essential that the basic transmission channel parameters be known for the development of suitable equalization procedures.

Different approaches can be envisioned each requiring a different list of parameters to define the transmission channel. In this report the concern is with the basic wideband measurement of the time-varying impulse response on a continuous basis over representative intervals. Measurements should be performed in the higher frequency bands now, in order to avoid serious EMI problems that will be encountered when allocations are made for use of the bands. Response data obtained now (where channels are still clear) at several locations and at different carrier frequencies and recorded on magnetic tape would provide an extremely useful data bank. The various analysis procedures could be applied at any time to meet future requirements.

Mobile radio channels can be characterized by measuring the time-varying impulse response and then determining the time-frequency correlation functions. This is fairly common practice by other workers; see Cox (1972b) as an example. In this report we describe the capabilities of the Institute for Telecommunication Sciences (ITS) for this type of channel characterization. The ITS capabilities are demonstrated through measured examples of some mobile channel responses obtained in Boulder, Colorado, using a pseudo-random noise (PN) channel probe described in Section 2. Data processing techniques available in the ITS laboratory are also described. These techniques are ideally suited to characterizing land-mobile problems.

2. THE ITS CHANNEL PROBE

The impulse response h(t) of a radio channel at a given instant in time is defined as the channel output when a unit impulse or delta function $\delta(t)$ is impressed on the input. Given h(t), any arbitrary input x(t) produces an output y(t) given by the convolution integral:

$$y(t) = \int_{-\infty}^{\infty} x(\tau)h(t-\tau)d\tau = x(t) \boxtimes h(t) \qquad (1)$$

where $\boxtimes$ denotes convolution. Note that the convolution of a function f(t) with the unit impulse $\delta(t)$ yields the function itself as

$$f(t) \boxtimes \delta(t) = f(t). \qquad (2)$$

One obvious way to measure the impulse response of a channel is to transmit a unit impulse through it and observe the output response. However, it is only possible to approximate a unit impulse in practice. The width of the pulse actually used must be much less than the response time (reciprocal of the bandwidth) of the channel of interest. An alternate method is to use impulse-type functions which take advantage of time-bandwidth tradeoffs (Hubbard, 1971). If the input to the filter x(t) has an autocorrelation function given by:

$$R_{xx}(\tau) = \frac{1}{T}\int_0^T x(t)x(t+\tau)dt \ , \qquad (3)$$

then the cross correlation of the output with the input

$$R_{xy}(\tau) = \frac{1}{T}\int_0^T y(t)x(t+\tau)d\tau \ , \qquad (4)$$

is also given by

$$R_{xy}(\tau) = \int_{-\infty}^{\infty} h(t-\tau)R_{xx}(\tau)dt = h(t) \boxtimes R_{xx}(t). \qquad (5)$$

The cross correlation $R_{xy}(\tau)$ yields the impulse response h(t) when the input is a white-noise source, since for white noise

$$R_{xx}(\tau) = \delta(\tau) \tag{6}$$

$$R_{xy}(\tau) = h(t) \otimes \delta(\tau) = h(\tau) \tag{7}$$

Although the white-noise source provides an ideal signalling format, it presents problems in practice because the broadband spectrum may cause interference to other users (nearby channels), and because it cannot be duplicated at separate terminals. It is possible, however, to use pseudo-random noise (PN) in a binary key stream. The autocorrelation function of such a signal approximates the unit impulse over a more limited bandwidth.

Pseudo-random keystreams which satisfy most of the randomness properties, and have an autocorrelation function similar to that of bandlimited noise can be generated using a maximum-length sequence generator. Such a generator consists of n consecutive binary storage units, a clock which shifts the state of each storage unit to the next, and two exclusive "or" feedback loops. The output of the generator consists of a series of rectangular wave forms which ultimately repeat in sequence at periodic intervals of $\Delta\tau = (2^n-1)\Delta t$, where n is the number of storage units and Δt is the clocking period. This is the basic concept used in the ITS channel probe employed for measuring mobile channel characteristics at 8.6 GHz. A detailed description of the probe and measurement techniques is given by Linfield et al., (1976), and summarized below.

The ITS channel probe consists of a transmit terminal and a receiver terminal with appropriate antennas for each, and with equipment for data recording and display.

A block diagram of the transmit terminal is depicted in Figure 1. This system transmits a carrier that is phase modulated by the PN binary bit stream. The PN code is generated from a 9-stage shift-register, providing a repetitive sequence 511 bits long and clocked at 150 MHz. The autocorrelation function of this keystream is triangular in shape, and is slightly more than 13 ns in width at its base.

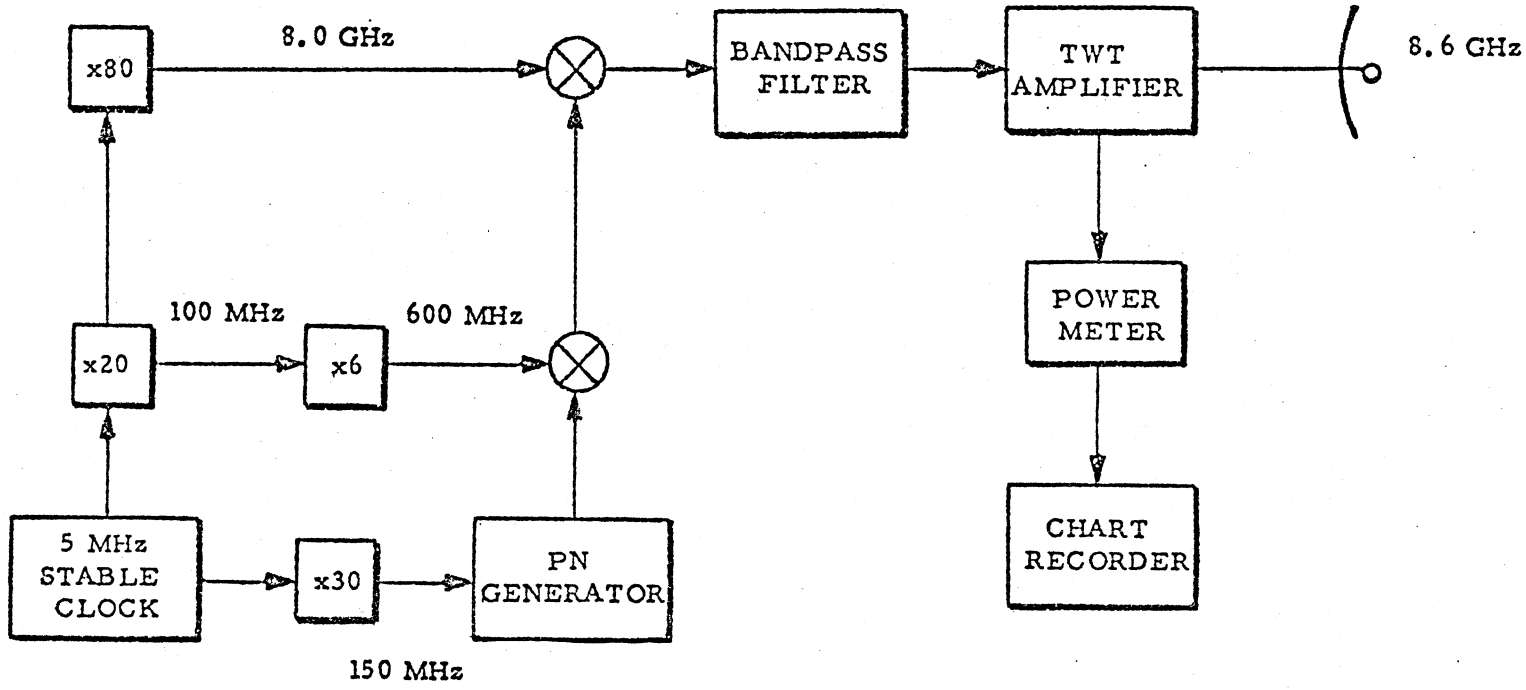

Figure 1. Block diagram of the ITS Channel Probe transmitter.

A 5 MHz stable oscillator provides a reference frequency to develop both a 600 MHz IF and an 8 GHz rf carrier signal. The 600 MHz IF signal is biphase modulated with the pseudo-random sequence and mixed in a double balanced circuit with an 8 GHz signal to produce a double-sideband suppressed carrier signal, with the two sidebands centered at 7.4 and 8.6 GHz. An rf filter is used to pass the upper and reject the lower side-band. A traveling wave tube (TWT) rf amplifier provides the signalling power (up to 20 watts) to the antenna via a low loss transmission line.

The receiver terminal block diagram is shown in Figure 2. The received signal is correlated with a co- and quadrature-phase replica of the transmitted signal, at the IF of 600 MHz. These quadrature functions permit the relative phase of the received multipath components to be determined. The quadrature functions are also squared and summed to provide a direct output of the power envelope of the impulse. In addition, the 600 MHz IF signal is monitored on a power meter and may be recorded through a log converter amplifier for the received signal level (RSL) measurement.

The receiver terminal includes a self-calibration feature. A locally generated 8.6 GHz pseudo-random modulated signal identical to that generated in the transmit terminal is available in the rf head of the system. Step attenuators in the rf head are used to calibrate the receiver output using this known signal at the input.

The characteristics of the probe as used for the mobile channel measurements described in subsequent sections of this report are listed in Table 1.

The modular construction used in the probe permits modifications to be made easily to meet a variety of requirements or channel conditions. Table 2 lists the range of transmission frequencies and power, PN code parameters, and antennas which have been used.

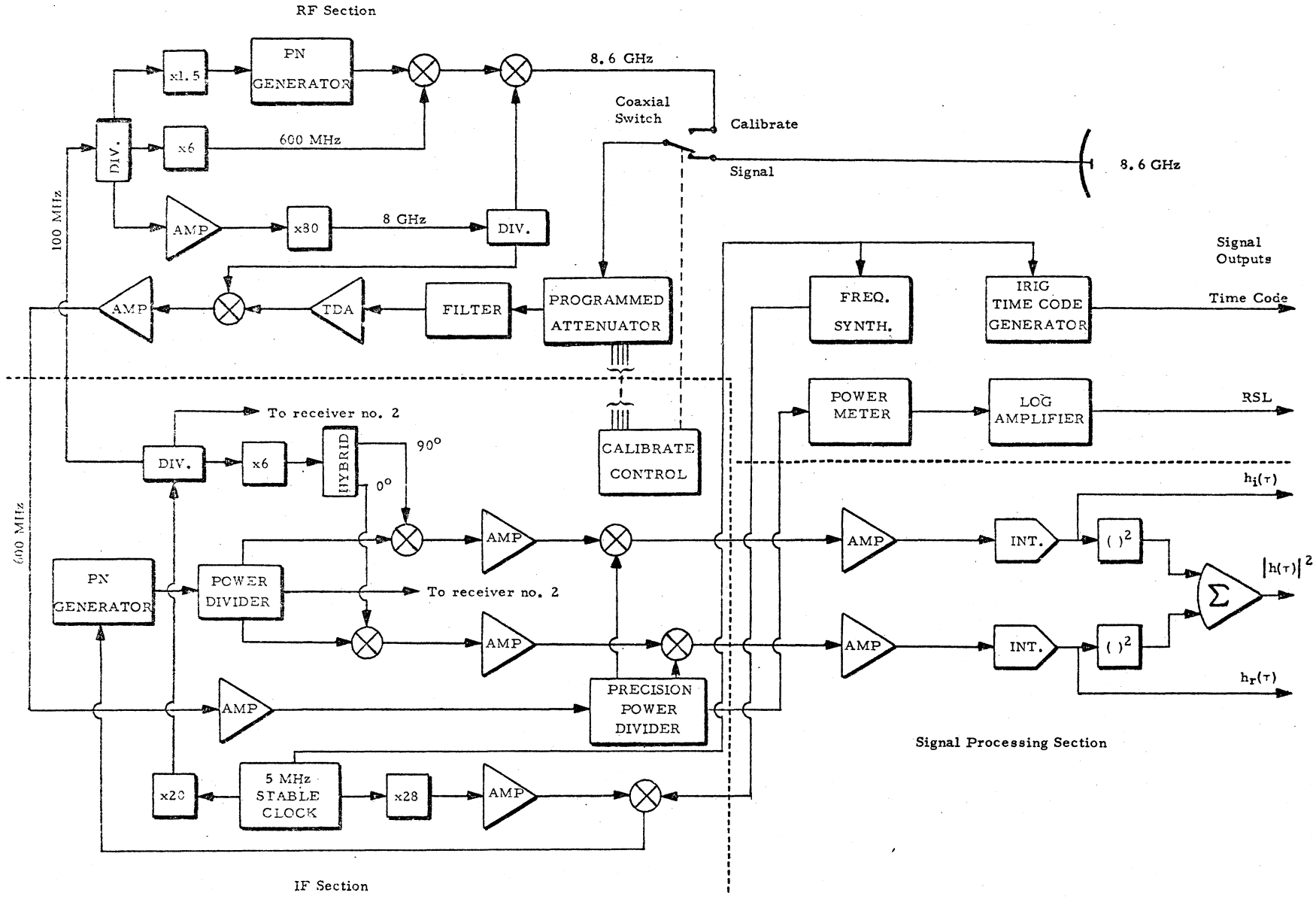

Figure 2. Block diagram of the ITS Channel Probe receiver. Output signals are recorded on paper strip chart and/or magnetic tape.

Table 1

ITS Channel Probe Characteristics
For The Land-Mobile Measurements

Transmitter	
Reference Oscillator:	5 MHz
IF Frequency:	600 MHz
Pseudo Random Key Stream Generators:	9 Stage
PN Code Length:	511
PN Clock Rate:	150 MHz
Modulation:	Bi-phase Single Sideband
Carrier Frequency:	8.6 GHz
Transmitter Power Amplifier:	20 watt TWT
Antenna:	Standard Gain Horn
Polarization:	Vertical
Antenna Gain:	20 dB
Beamwidth:	~20 degrees (3 dB)
Positioning:	Manual
Receiver	
Antenna:	$\lambda/4$ Stub Above Ground Plane
Gain:	~3 dB
Beamwidth:	Isotropic
Polarization:	Vertical
Preamplifier:	Tunnel Diode
Gain:	17 dB
Noise Figure:	≈10 dB
Bandwidth:	300 MHz
Reference Oscillator:	5 MHz
IF Frequency:	600 MHz
Dynamic Range:	≈20 dB (range selectable)
Calibration Signal Level:	-54 dBm (Nominal)
PN Generation:	511 Bits-Adjustable Rate
Display:	Calibrated Oscilloscope
Recorders:	Magnetic Tape and 2 Channel Chart
Data Signals:	a. Impulse Envelope Power b. Co-Phase Impulse c. Quad-phase Impulse d. IF Output, Log-Linear RSL e. Time Code (IRIG), Code E f. Synchronizing Signal

Table 2

Summary of PN Probe Transmission Capabilities

Freq. Band	IF MHz	Typical PN Code Rates (MHz)	Transmitter Power		Available Antennas
			Low	High	
L	70	50	1 W	300 W	(a) Standard gain horns
			1 W	200 W	(b) λ/4 Stub
S	70 or 600	10 to 150	1 W	150 W	(c) 6' Parabolic
			1 W	1 KW	(d) 10' Parabolic
			1 W	20 W	(e) 60' Parabolic fixed position-beyond horizon path
X	70 or 600	50 to 150	1 W	20 W	

Note: The PN code length is variable from 7 to 32,767 bits (n = 3 to 15)
Nominal code length = 511 bits (n = 9)

Figures 3a and 3b are photographs of the transmit and receive terminal equipment. The transmit terminal consists of two 5½-inch rack mounted chassis; one is the signal generator and the other is a TWT power amplifier. The receive terminal consists of an rf unit, an IF unit, and the signal processing unit. All can be easily carried and operated in a small station wagon or van equipped with a small power generator.

3. MEASUREMENT PROCEDURES

The PN probe receiver was mounted in a mobile van equipped with an integral power generator. Data logging facilities included a variable persistance scope (from which polaroid photographs of the response could be obtained) and a portable magnetic tape recorder. The receiving antenna was a nominal quarter-wave vertical stub above a ground plane, mounted on a mast approximately one meter above the roof of the van on the rear.

The transmitter was housed in a closed equipment rack, and secured to a concrete pad on the east edge of Green Mountain, behind the Department of Commerce (DoC) laboratories. The transmitter antenna was a standard-gain horn with a 3 dB beamwidth of approximately 20° azimuth, and a gain of 21 dB above an isotropic radiator. The horn was mounted on a pipe mast approximately 3 m above the surface. The mast could be conveniently rotated to orient the antenna to any desired azimuth angle. Measurements were made with the receiver van at distances from 1 to 5 km from the transmitter. For each run, the transmitter antenna was oriented in azimuth such that the receiver van essentially remained within the azimuth beamwidth.

Measurements, made in four general areas within the City of Boulder, Colorado, can be described as follows:

1. Residential streets.
2. Areas with single-family homes, open-space (parks and lakes) and high-rise apartment buildings.
3. Downtown business area, with buildings ranging from one to eight stories in height.

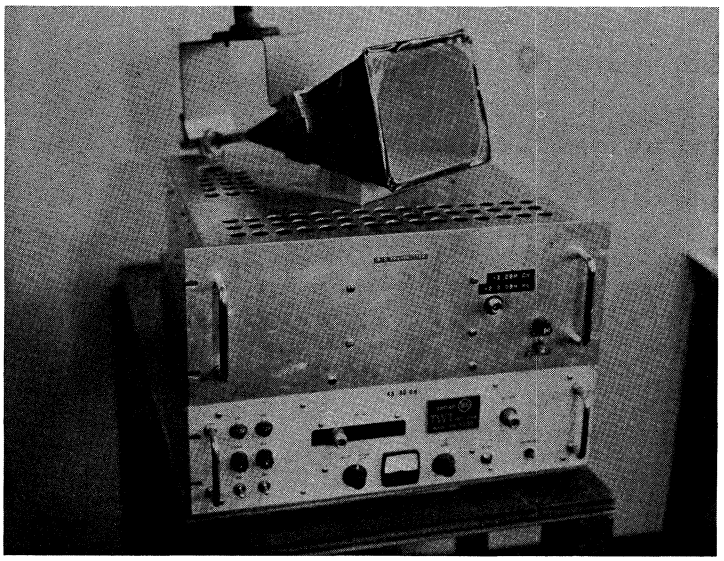

(a) PN transmitter, showing the standard-gain horn antenna.

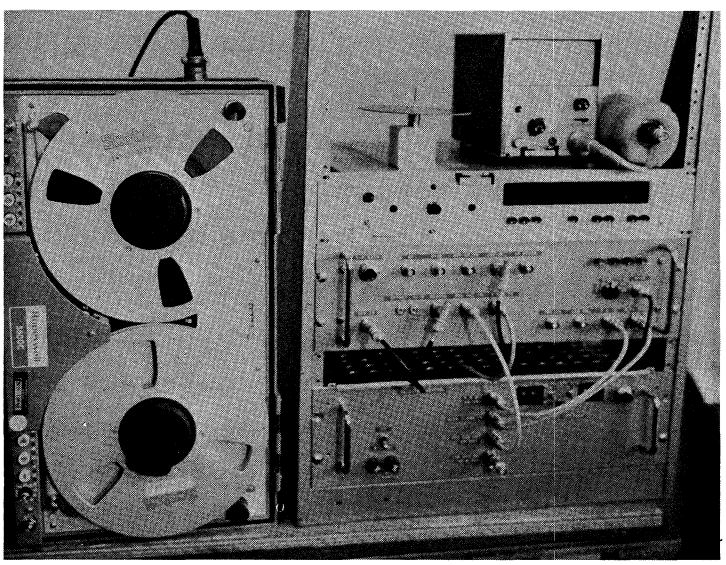

(b) PN receiver with magnetic tape recorder.

Figure 3. The ITS PN Channel Probe.

4. Streets forming state and Federal highways through the city, with a mixture of business buildings and shopping centers.

Examples of the measured results from most of these regions are presented in Section 5.

All measurements were recorded on magnetic tape, and included the following data signals:

1. IRIG time code.
2. $|h(t)|^2$ - linear scale.
3. $|h(t)|^2$ - log scale.
4. Synchronization pulse derived from the PN code length.
5. Voice annotation describing van location and features of the vicinity.

The data rate for the probe was selected to provide impulse response windows at the rate of 10 per second (100 ms/window). A code length of 511 bits at a clock rate of 150 MHz was used. Thus, each correlation window provides a maximum delay time measurement of approximately 3.4 μs. In this case, the time scaling factor is nearly 30,000*; 1 ms in data display-time represents approximately 34 ns in real time. This data rate was observed to be adequate, even when the van was in motion, since no significant change in the time-delay structure of the measured response could be detected in adjacent windows. The observation illustrates that the time variability of the data was slow compared with the selected data rate at the vehicle velocities used (5 to 15 mph).

4. ANALYSIS PROCEDURES

The magnetic tapes were returned to the laboratory for processing and analysis. Each tape was scanned for times of most

*This scale factor is six times that used by Cox (1972a), who states that a factor of 5,000 yields only slight distortion to the correlation pulse.

significant data in relation to the regions described in the previous section. Selected periods were analyzed, and the results are presented below.

The time-domain impulse response provides an immediate display of the multipath structure of a transmission channel. It measures both the relative path delays (and consequently the path length differences) and the relative magnitudes of each path response. In reality, this function contains more information than can be easily used to predict system performance although it is ideally suited for the "stored channel" simulation process as described by Bussgang, et al. (1976). The function is time-variant, and can change quite rapidly in the land-mobile channel as one or both terminals are in motion. The dynamic channel affects on a variety of information signals could be determined from a laboratory simulator, where the measured responses form the time-variant kernel in a real-time convolution process given by (1). Other approaches include using the measured data as time-sampled functions that then describe the appropriate tap-gain functions for a tapped delay-line model of the channel. These methods are the only way in which dynamic effects of the channel functions can be measured in the laboratory.

Many authors (Kailath, 1959; Gallager, 1964; Cox, 1972a and b; and Bello, et al., 1973), however, have illustrated the utility of various statistics of the channel functions in providing an evaluation of the average of communication capabilities in the channel. One of the more useful statistics is that of the two-frequency correlation function given by

$$R_H(\Delta f,\Delta t) = \chi\,[H(f,t)\ H(f+\Delta f,t+\Delta t)] \qquad (8)$$

where χ denotes the correlation integral. This as well as other statistical characteristics of the channel are discussed in a good, general treatment by Gallager (1964). There are two special cases of (8) to consider. First, we note that for $\Delta f=0$, $R_H(0,\Delta t)$ is the correlation of the system transfer function for a

sinusoidal input. From this, the coherence time of the channel can be derived. The second case is given for $\Delta t=0$, in which $R_H(\Delta f,0)$ is the correlation of the transfer function over a broad band of frequencies and is a function of Δf. For example, this correlation function is given by

$$R_H(\Delta f,0) = R_H(\Delta f) = F\left[h(t,\tau)h^*(t,\tau)\right] = F\left[|h(t,\tau)|^2\right] \quad (9)$$

where $F[\cdot]$ denotes a Fourier transform operation, * denotes a complex conjugate, and $h(t,\tau)$ is the equivalent low-pass impulse response function of the channel (response at time t to an impulse applied at the input τ seconds earlier). Note that the quantity in the brackets of the final expression of (9) is the measured function from the channel probe.

The relation given by (9) is of primary interest here, and represents the analysis performed on the measured data. However, before presenting these results, it is informative to examine some additional relationships between the measured functions from the probe and other statistical functions found in the literature.

Taking inverse Fourier transforms over Δf on both sides of (9), and noting by definition that

$$R_h(\tau,\Delta t) = F\left[R_H(\Delta f,\Delta t)\right], \quad (10)$$

we find for the special case $\Delta t=0$

$$R_h(\tau) = |h(t,\tau)|^2. \quad (11)$$

The correlation function of (10) is commonly referred to as the tap-gain correlation function. It is obvious from (11) that the probe yields a direct measure of $R_h(\tau,0)$, and consequently, the multipath spread (or smear) of the channel.

The doppler spread of a channel at any arbitrary delay τ can generally be determined from a measure of either of the correlation functions given by (9) or (10) over the variable Δt. The interval in Δt where these functions are effectively nonzero is the same, and as noted before, this is a measure of the coherence

time of the channel response. The doppler spread has the order of magnitude of the reciprocal of the coherence time. There is also a third characteristic function defined as the scattering function of a time- and frequency-spread channel. This function is similar to the transform of (10), when the operation is taken over Δt. The range in f where the scattering function is effectively nonzero is a direct measure of the doppler spread.

It should be noted from (10) and (11) that data recorded from the probe measurements can be processed from the magnetic tapes in computer routines to derive the scattering function. This process however is beyond the scope of this report.

From (9) we note that the special case of the two-frequency correlation function is obtained directly from a Fourier transformation of the measured data. In the results reported by Cox (1972a and b), this transform was calculated by hand. The OT/ITS has in its laboratories a time-series analyzer ideally suited to processing these data. The system is a digital computer in which all the basic time-series analysis algorithms are hardwired into the program. Selection of any algorithm is made from a push-button on the computer console. The analyzer is an all-digital processor, capable of accepting input data in either analog or digital form, and also providing output functions in either format. Analog inputs are converted by an integral A/D interface; analog outputs are developed from an integral D/A interface. Output data plots can be provided through digital recording at the output, and processed in a large-scale computer with CRT routines, or directly from the system on an x-y recorder.

One of the selectable algorithms on the above analyzer is the Fourier transform and its inverse. Input data are block oriented, and the output is developed in two quadrature components representing the real and imaginary parts of the transformed function. Each of these components is displayed in a data block equal in length to that of the input function, and stored in output buffers. Another selectable algorithm is that of real or complex multiplication. Data may be readily transferred

in block mode from output to input buffers (or vice versa) at the discretion of the operator. Thus, compound operations may be quickly performed within the computer. For example, in our processing routine, the complex result of the Fourier transform of the time function is transferred back to input buffers and processed again in the multipliction algorithm. The result of this operation is then the correlation function desired from the process given in (9).

For the special case of (9), it can be shown that the transform of the power impulse response also represents the magnitude-squared value of the frequency transfer function. This provides additional insight on the transmission quality of a given channel. Examples of measured values and the transform analyses are presented in the following section.

Before presenting specific data samples some general observations are appropriate. First, the direct-path signal was present and undistorted whenever the transmitting site could be seen, unobstructed, from the van. Conversely, if the visual path between the van and the transmitter was blocked, even by relatively small trees, for example, the direct path was severely attenuated. Second, when the van was stopped, the responses indicated one or more distinct paths with no noticeable spreading of the individual pulses. However, when the van was moving, it was not unusual to see a spreading, or superposition of the delayed pulses, but this was rarely seen for the direct pulse.

In the following sequence of figures, the length of the window observed corresponds to 3.4 μs total delay time. These responses were recorded at 10 windows/second. These data were played back at different speeds, and recorded on charts at different speeds to illustrate the different types of data observed. No attempt was made to obtain a precise calibration for these illustrations because of the response time and overshoot of the chart recording. Generally, however, full-scale for the time-expanded playbacks is 33 dB.

Figure 4 illustrates three different time scales from a segment of data when the receiver van was moving. The delay between the direct pulse and the largest reflected pulse is ~400 ns.

Figure 5 shows two samples, the first representing delays between 25 ns and 45 ns and the second, a delay of 870 ns. The second sample was taken with the van stopped. That sample shows the typical lack of distortion of impulses. Figures 6 and 7 show additional samples of data taken with the van moving. The middle trace in Figure 7 shows the direct signal attenuated by a small tree approximately 50 meters from the van, while the signal reflected from a building behind the van is not attenuated. The delay times are as noted on the figures.

Figure 8 shows a sequence of windows during which time the van was moving toward the transmitter and away from the reflecting building. The delay spread changes form 217 ns to 275 ns, corresponding to a speed of ~17 mph (27 km/hr) for the van.

Figure 9 shows the time history for three different moving configurations. The approximate delays are 180 ns, 300 ns and 1.25 μs for the charts from top to bottom, respectively. The first two samples were recorded in a situation where the van was moving parallel to the reflecting building, with utility poles between the van and transmitter. For the third sample, the van was moving toward the transmitter and away from the reflecting building at about 2 mph (3 km/hr).

5. ANALYSIS RESULTS

In this section we present a representative sample of the land-mobile transmission channel measurements made in Boulder, CO. Examples of each of the regions noted in Section 3 are included, with the exception of residential streets. At the high microwave frequency used for the measurements (8.6 GHz), these areas were found to be of little interest because the residential streets are heavily tree-lined, and the direct signal was attenuated by trees and buildings in most areas. Multipath signals

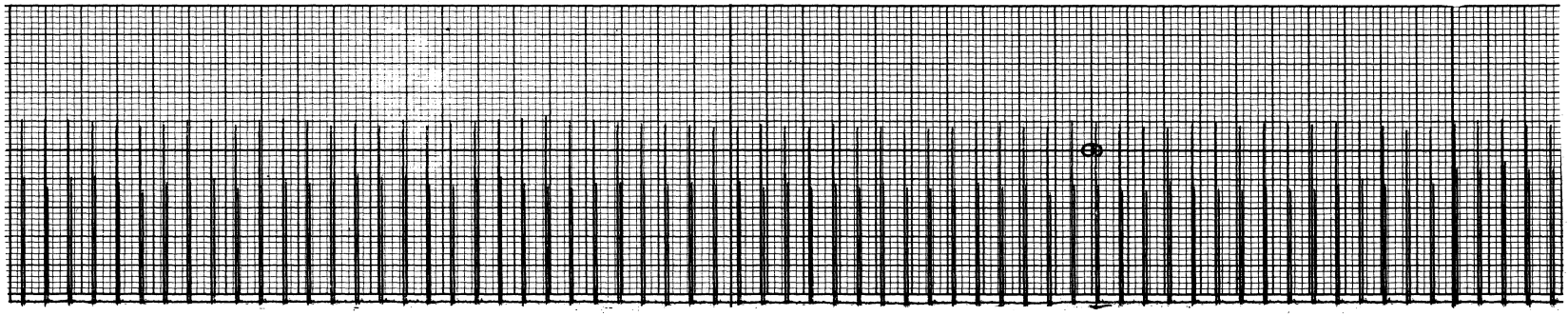

Sequence of measured impulse responses; 3.4 μs time delay for each response window.

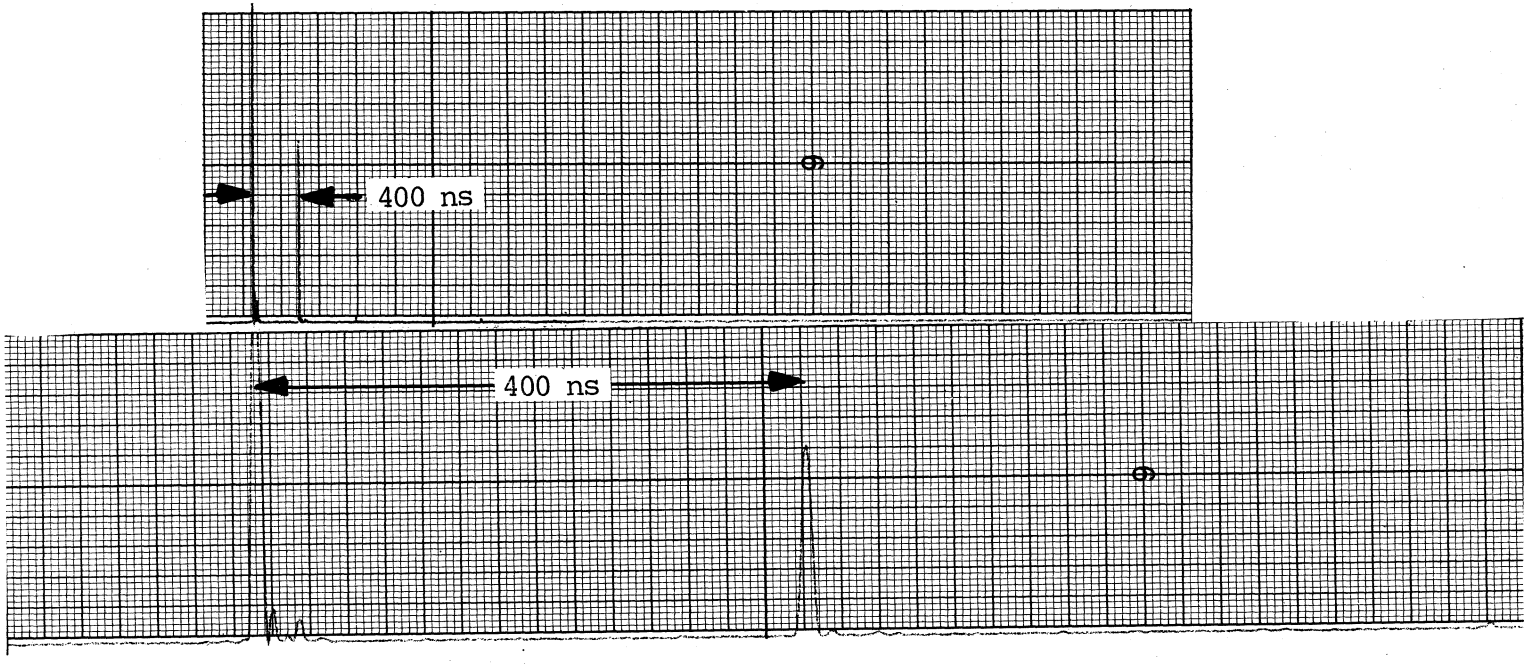

Figure 4. Three time scales for the same run of data, each showing different details of the impulse response; the delay between the direct and largest reflected pulse is 400 ns.

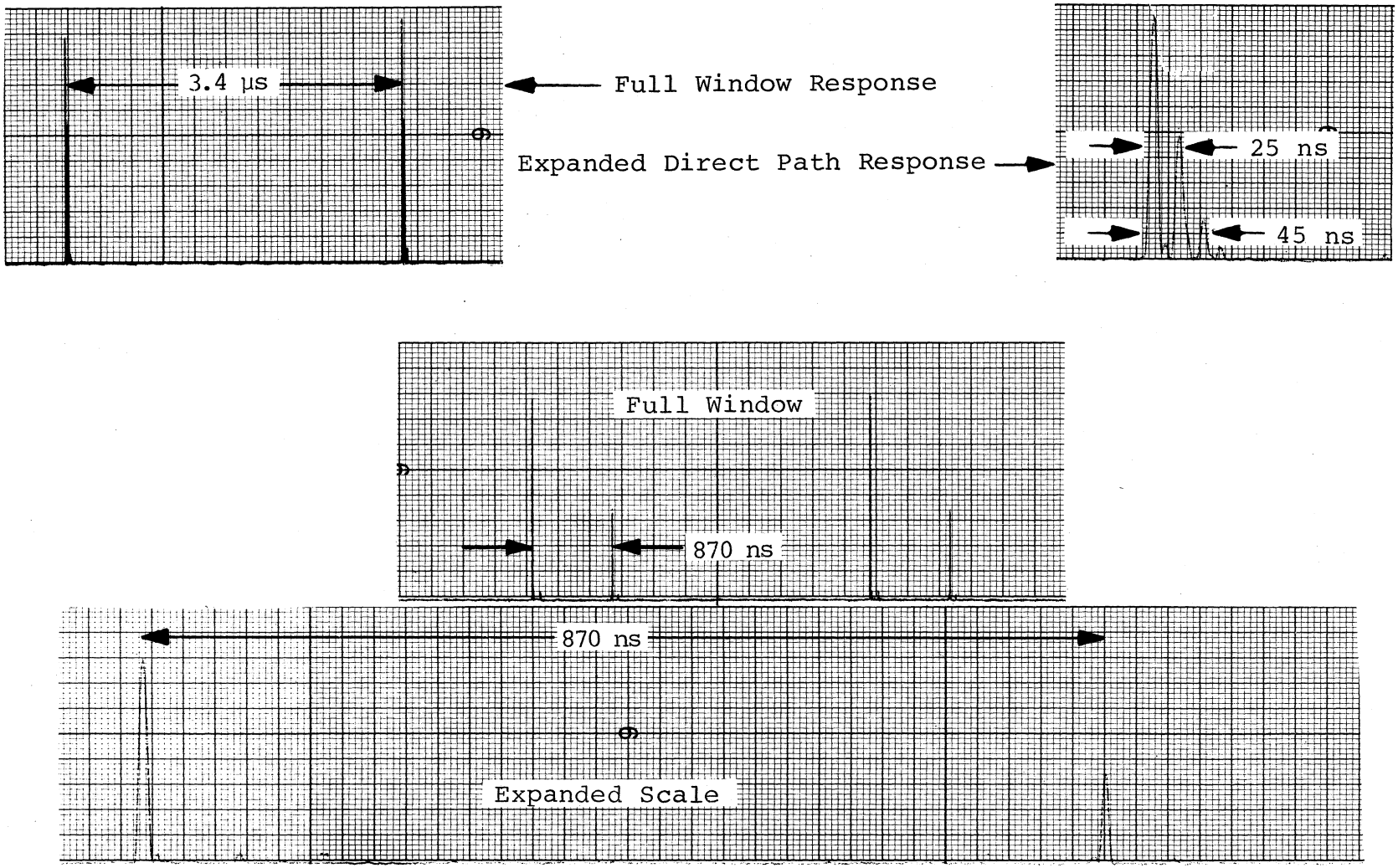

Figure 5. Top trace: a sample showing general delayed returns between 25 and 45 ns after the direct response. Middle and bottom trace: a sample, with the van stopped showing a delay of 870 ns. Note the lack of distortion in the impulses.

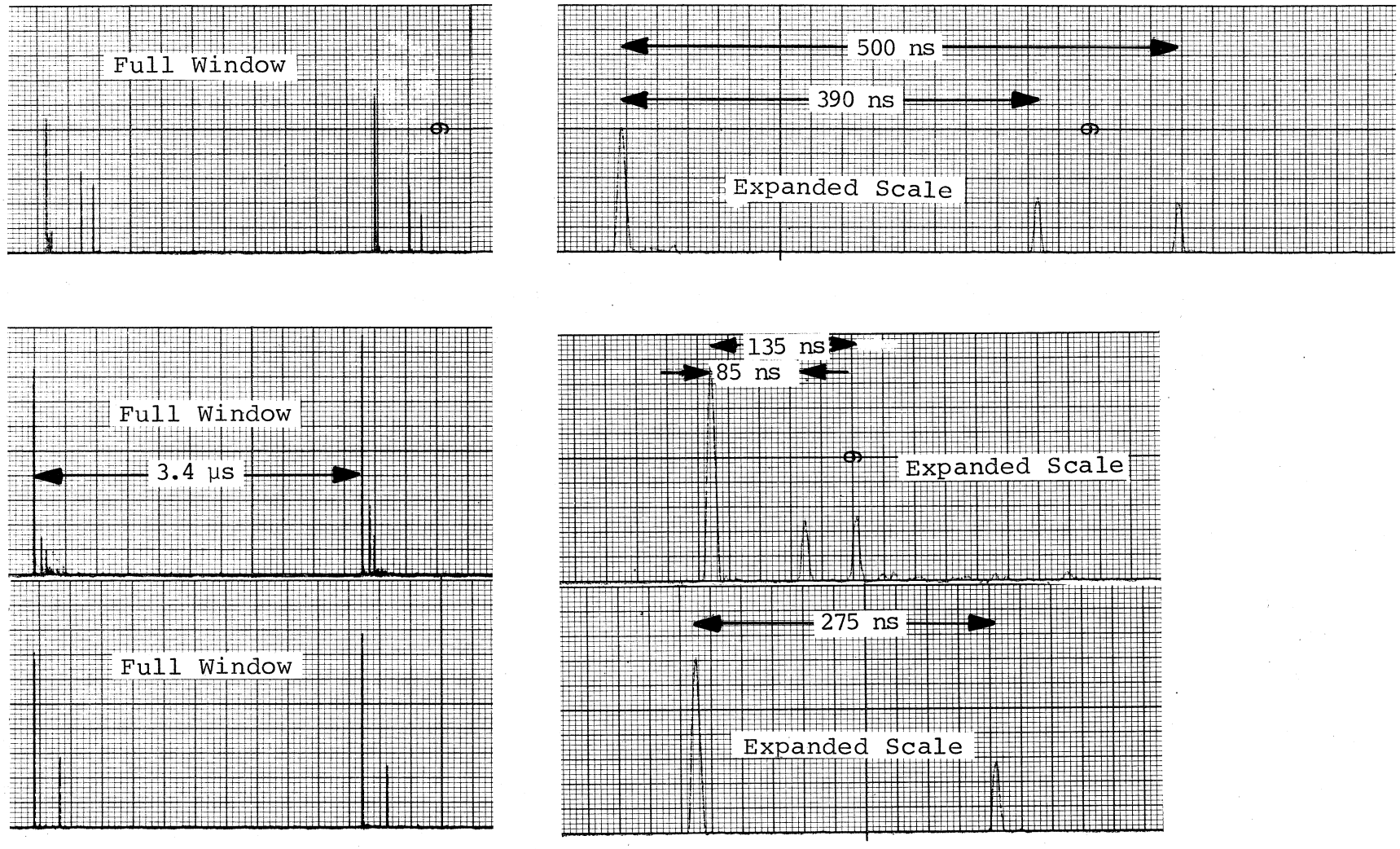

Figure 6. Samples of impulse responses with the van moving. The delay times are as shown.

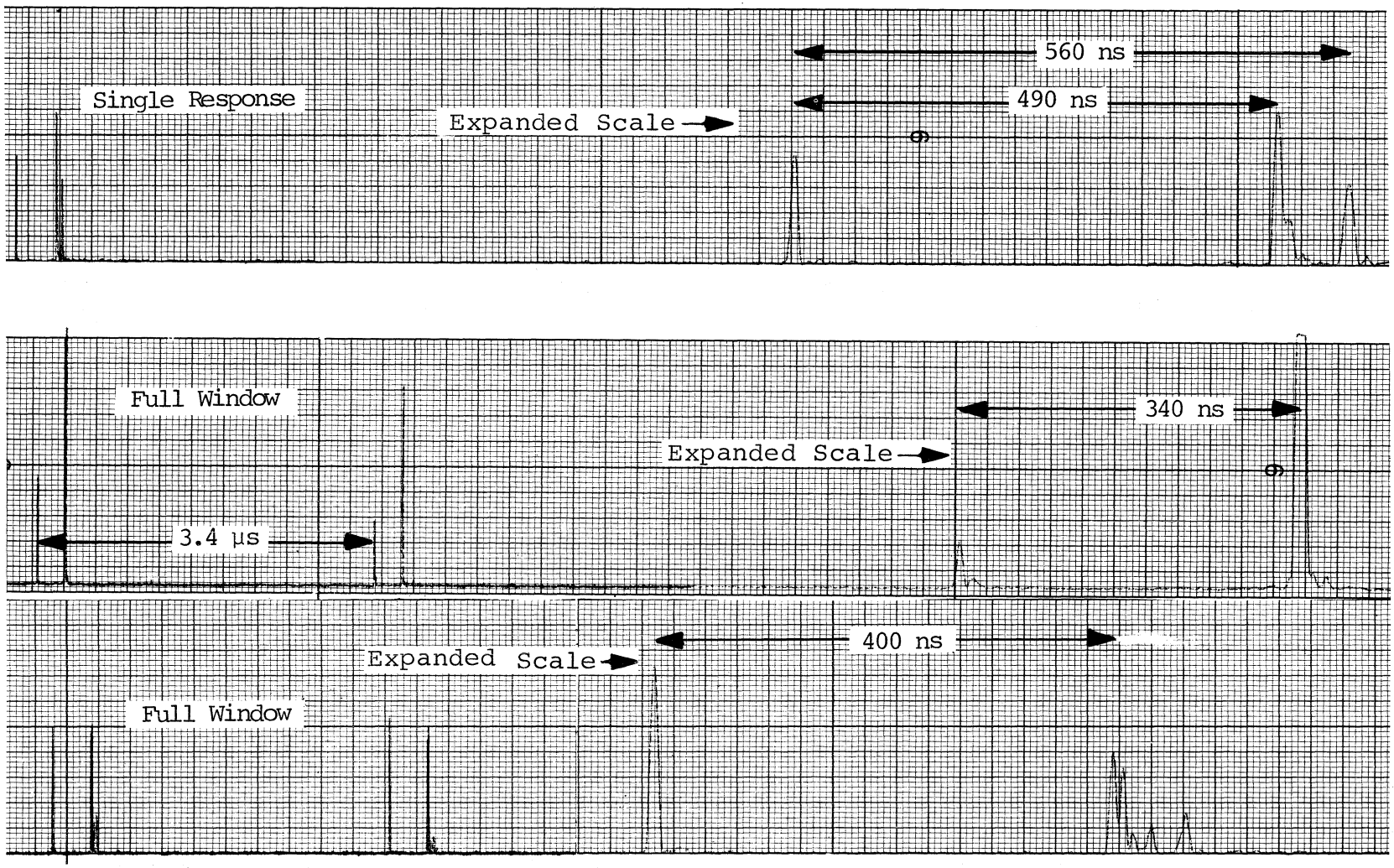

Figure 7. Samples of impulse responses with the van moving. The middle trace shows a sample with the direct ray blocked by a small tree.

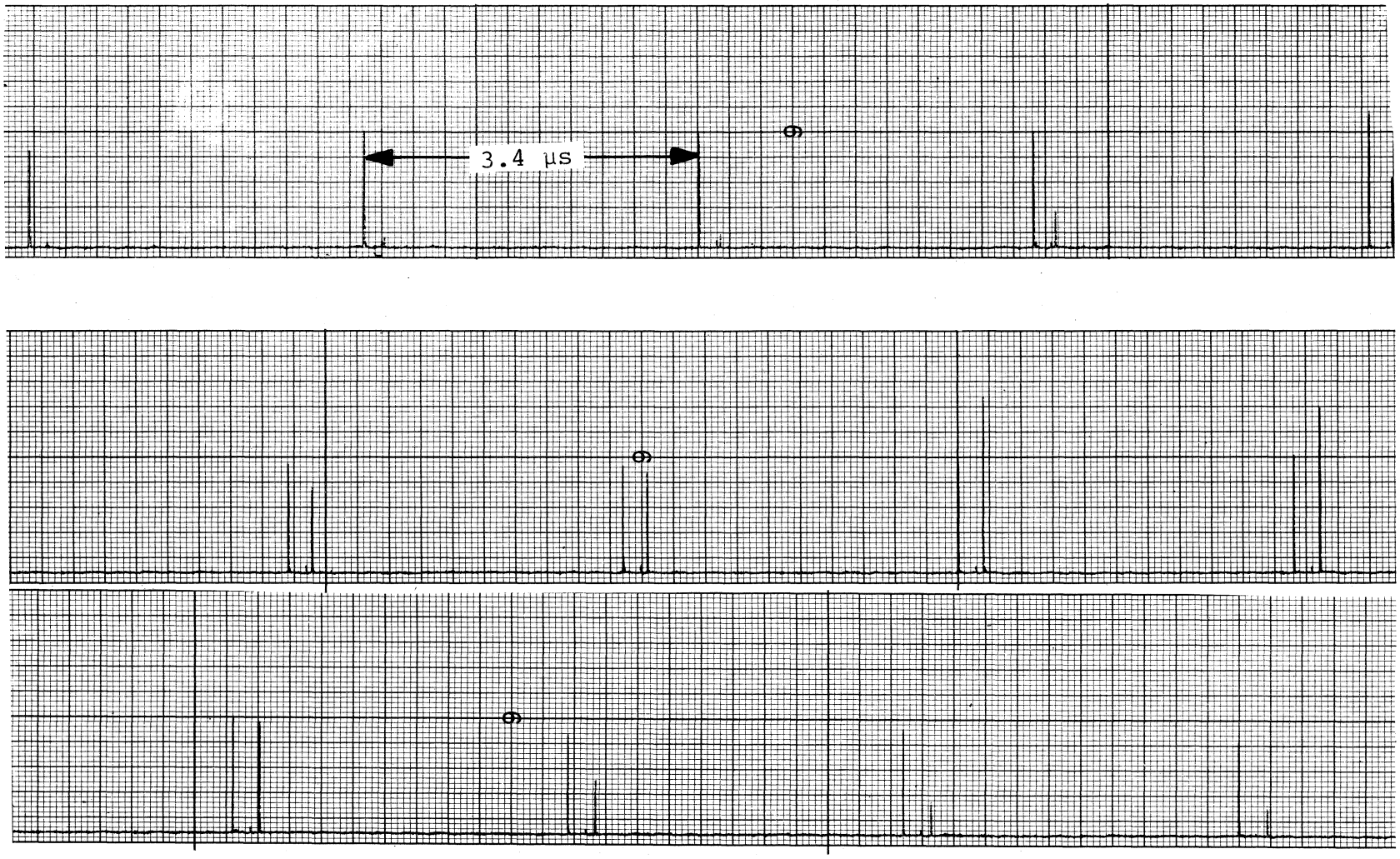

Figure 8. A sequence of impulse responses with the van moving toward the transmitter and away from a reflecting building. The delays range from 217 ns to 275 ns corresponding to a speed of 17 mph.

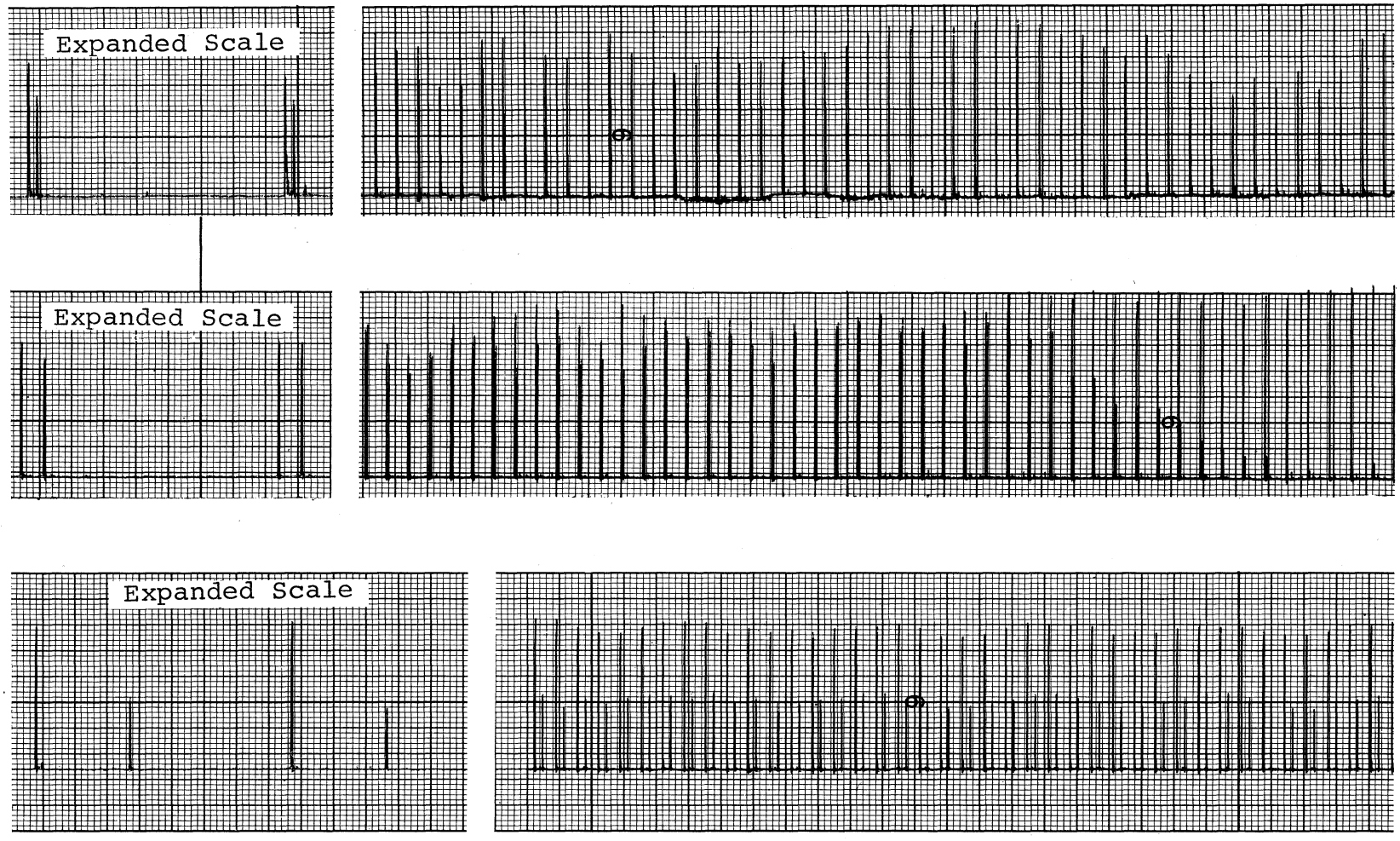

Figure 9. Three samples of impulse responses with the van moving. The delays are approximately 180 ns; 300 ns, and 1.25 μs from top to bottom respectively.

were seen in all cases; however, they were quite small and limited in delay time to the values expected for the path length differences between the receiver van and homes along the street.

5.1 System Calibration

In order to establish a reference level for the measured data, a measurement was made with the van positioned at close range and on a direct line-of-sight path to the transmitter. The recorded power impulse response is representative of a clear-channel (no multipath) and includes the effects of the measurement system, both transmitter and receiver. A typical calibration power impulse response is shown in Figure 10. Note that this short-path response is a fairly clean triangular function, with a slight multipath distortion at the base of the trailing edge. The plot has been made directly on an x-y recorder, at the output terminals of the time-series analyzer described in Section 4. In other words, the displayed impulse has been read from the magnetic tape recording, sampled in the A/D converter of the time-series analyzer, and plotted from an output buffer through the D/A interface. This general process has been used to produce all of the figures for the processed data included below.

The power impulse of Figure 10 was Fourier transformed in the analyzer. For illustration purposes only, the intermediate functions representing the real and imaginary parts of the transform process are shown in Figure 11. These functions are not included in subsequent results. The completed transform, representing the correlation function of (9) is shown in Figure 12. This result is seen to correspond very nicely to the theoretical frequency correlation function described by Cox (1972b). Note that the correlation decays to zero at a value of Δf = 150 MHz; the value of the PN clock frequency for the measuring probe. The fine-scale fluctuation on the function is a result of some quantizing noise in the analysis, and the small distortions in the time domain function (Figure 10) noted previously.

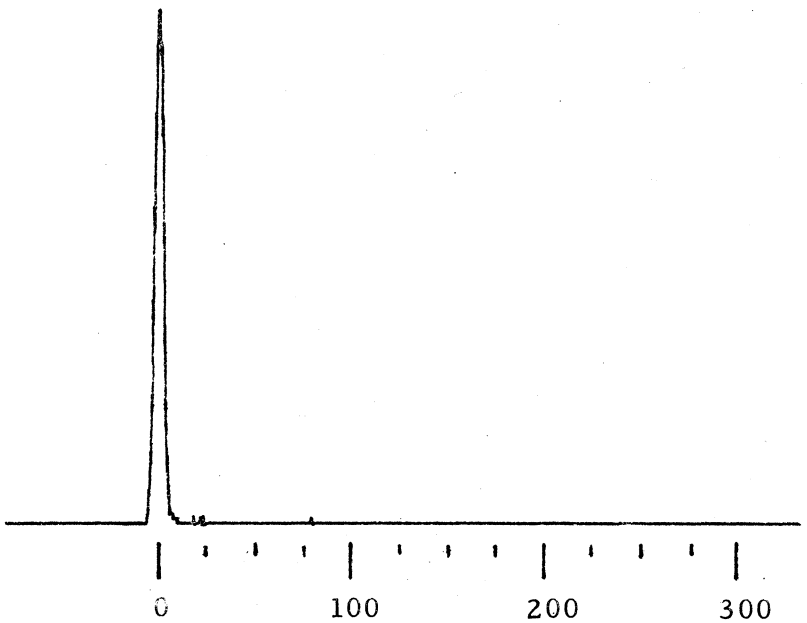

Figure 10. The impulse response used for calibrating the data presented in this report.

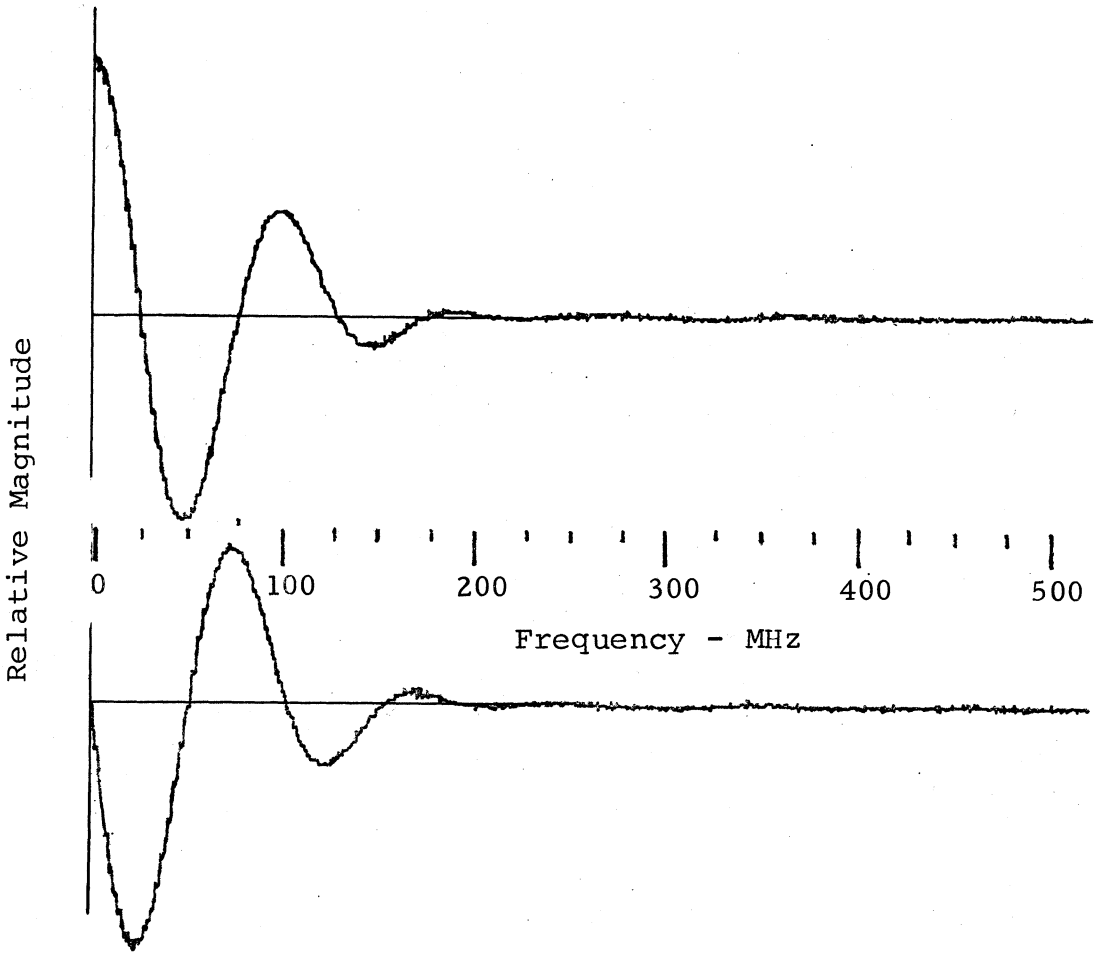

Figure 11. The real and imaginary components of the Fourier transform of the power impulse shown in Figure 10.

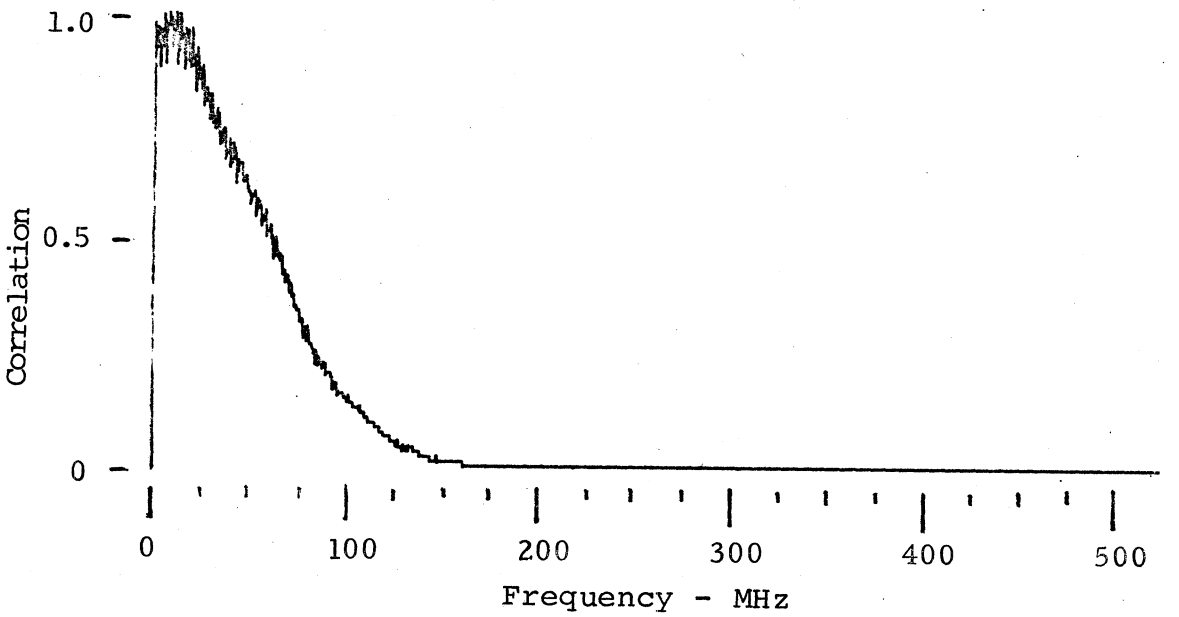

Figure 12. The frequency correlation function of the impulse of Figure 10. This function is the sum of the squares of the functions shown in Figure 11.

There is no absolute power calibration in these measurements. Since we are interested primarily in multipath, only relative magnitudes between direct-path and multipath components are important for the time-domain functions, and only the relative shape of the frequency correlation functions in the transformed data. Accurate received power calibration can be provided where desired, since the receiver contains a self-calibrating source as described in Section 2.

5.2 Measurements in Mixed Residential Areas

A few examples of the multipath measured in locations of mixed residential areas are discussed in this section. The location of the DOC Laboratories in Boulder is typical of these areas, where there is a mixture of residential streets, open space such as parks and greenbelt land, apartment houses, and is traversed by a major arterial street. The receiver van was located near the laboratory building when the multipath signal of Figure 13 was observed. The response in part a) of the figure shows two reflections (the first quite small) at delay times between 800 and 1000 ns. Figure 13b shows expanded-scale plots of both the direct path impulse and the multipath responses. These functions display the time resolution capability of the ITS probe. For example, note that the direct path impulse shows two short-delay components with small magnitudes near the trailing edge. The first of these is partially merged with the direct pulse (within the 6.6 ns resolution) but is distinguished by its peak value. The small reflection near 800 ns delay displays a rather dispersive character, while the larger response at the longer delay is quite specular.

The Fourier transform of this response is shown in Figure 14. The rapid fluctuation in the correlation function is a result of the delay component at 960 ns, which transforms to a cyclic term in Δf of slightly over 1 MHz. Thus, in this situation the coherence BW is on the order of 1 MHz. However, since the reflected component is approximately 0.4 times the magnitude of

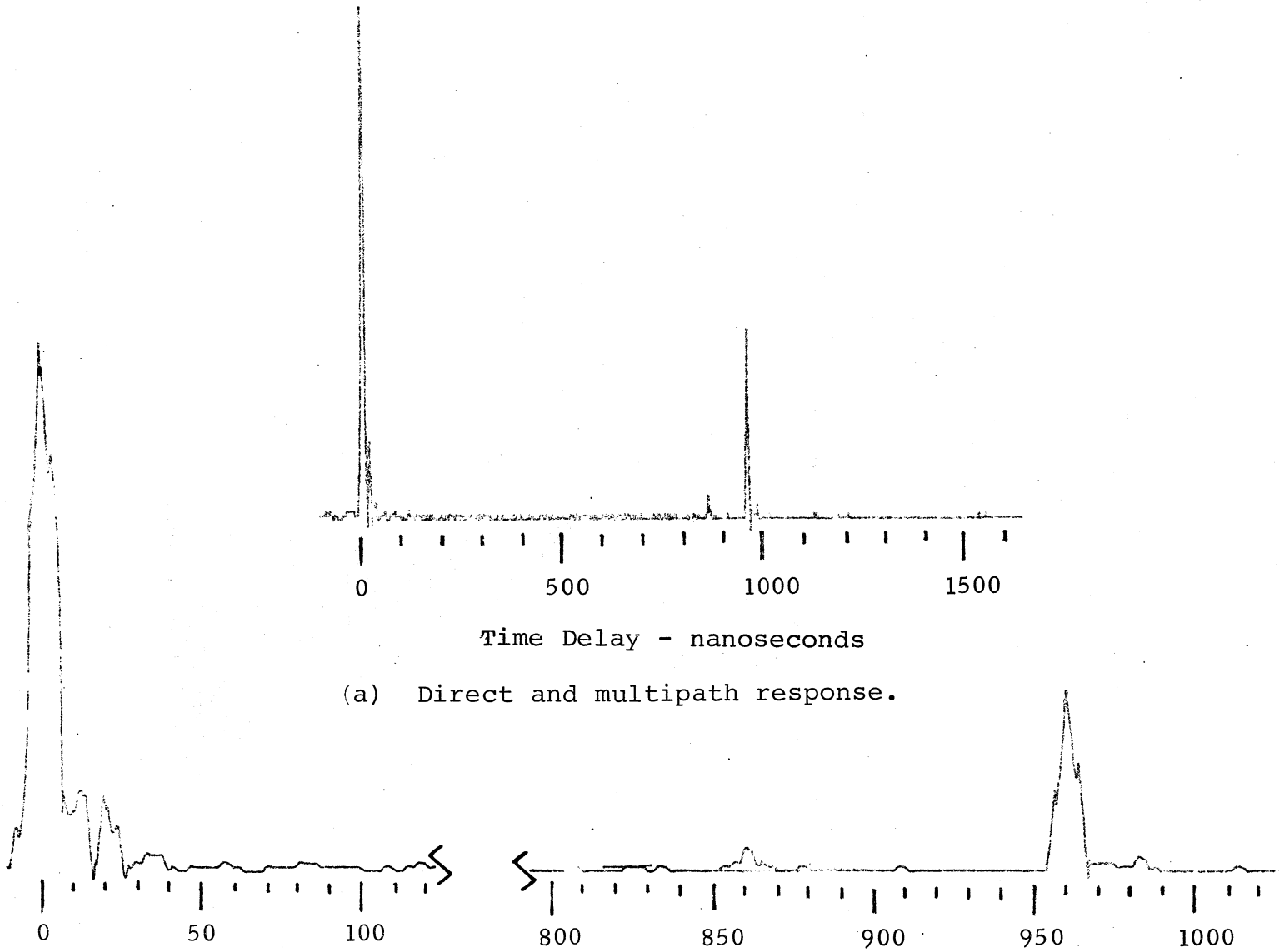

(a) Direct and multipath response.

(b) Expanded scale plot of (a).

Figure 13. An impulse response measured near the Department of Commerce Laboratories.

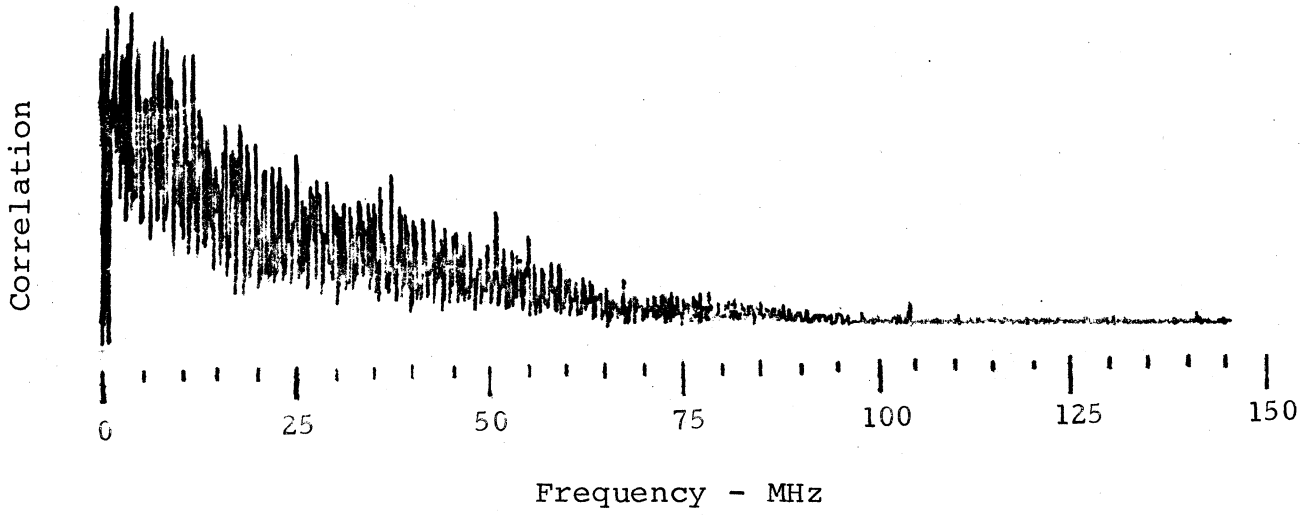

Figure 14. The Fourier transform of the impulse function of Figure 13 (frequency correlation function).

direct signal, complete cancellation (in the correlation function) does not take place over the complete range of the spectrum. For example, if we examine the lower limit of the envelope bounding the oscillatory part of the function, we note that the spectral energy is finite to frequencies of 60 to 65 MHz. The mean of the envelope extends to approximately 100 MHz. Comparing these features with the calibration function of Figure 12, we can conclude that the frequency transfer function $|H(f,t)|$ of this channel (at the instant of measurement) can be roughly characterized as sketched in Figure 15. The overall transmission band is limited roughly to 100 MHz by the short-term delay components (about 20 ns), and the envelope is scalloped over a range in $\Delta f \cong 2$ MHz. The latter characteristic is concluded from the fact that the frequency correlation function is derived from the magnitude squared value of the transfer function. Thus, the latter would be proportional (non-linearly) to the square root of the correlation function. The square root of a cyclic function yields a cyclic variation at half the frequency. Therefore, the scalloping in $|H(f,t)|$ would be twice the value of Δf observed in the correlation function. This example will serve to illustrate the information about the channel frequency transfer function that can be obtained from the correlation functions.

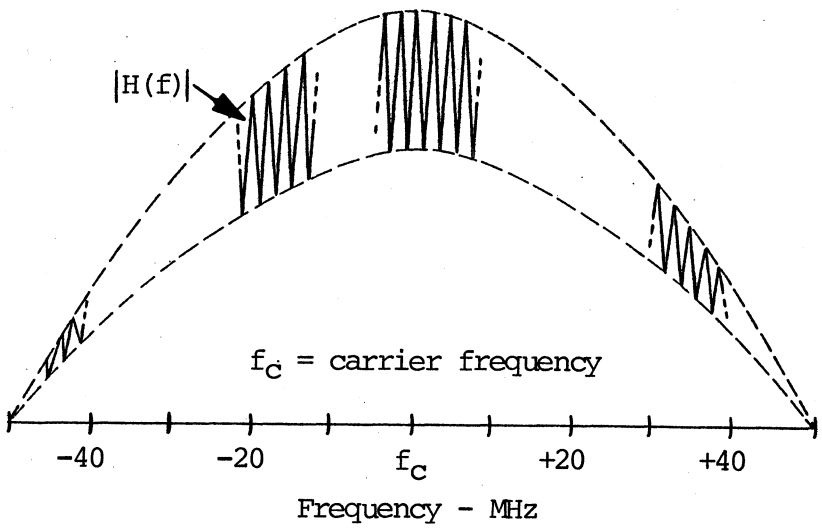

Figure 15. Theoretical frequency transfer function for the channel response of Figure 13.

Another response quite similar to that shown in Figure 13 above is shown in Figure 16(a). The path delays are seen to be less (520 and 580 ns) than the previous example, and the second reflected signal is seen to be slightly larger in magnitude than the direct signal. This response was measured in a mixed usage area of Boulder, where a small shopping complex, low office buildings, convenience stores, and a residential area merge at a major intersection (Baseline Rd. & 30th St.). Several high-rise dormitory buildings for the University of Colorado are located on the SE corner of this intersection. The receiver van was positioned in a shopping-center parking lot west of the dormitory buildings. It was determined (by using a hand-held metal reflector) that the large multipath component was a reflection from one of the dormitory towers. The smaller component is probably from some closer facet of the same building.

The Fourier transform of this impulse function is shown in Figure 16(b). Here again we see that the coherence BW is very small compared with the transmitter BW, and the rapid fluctuation corresponds to the long delay time. In this case the delay is about 580 ns for the large reflection, which transforms to a Δf fluctuation of approximately 1.7 MHz. This is roughly the spacing of the fluctuation peaks seen in Figure 16(b). Note also that the reflected component is actually larger in magnitude than the direct-path signal. Thus, the correlation function indicates periods of complete spectral cancellation across the transmission band. From an expanded scale plot of the impulse response (not shown) we can determine the delay spread of the direct response in Figure 16(a) to be on the order of 10 ns. Thus the transmission BW has been compressed to about 100 MHz, as can be seen from the spectral function of Figure 16(b).

The final example in this set is a response observed in a suburban area farther east of the Baseline Road-30th Street intersection. The receiver van was driven south of Baseline Road in the Thunderbird Development area. At one point the received

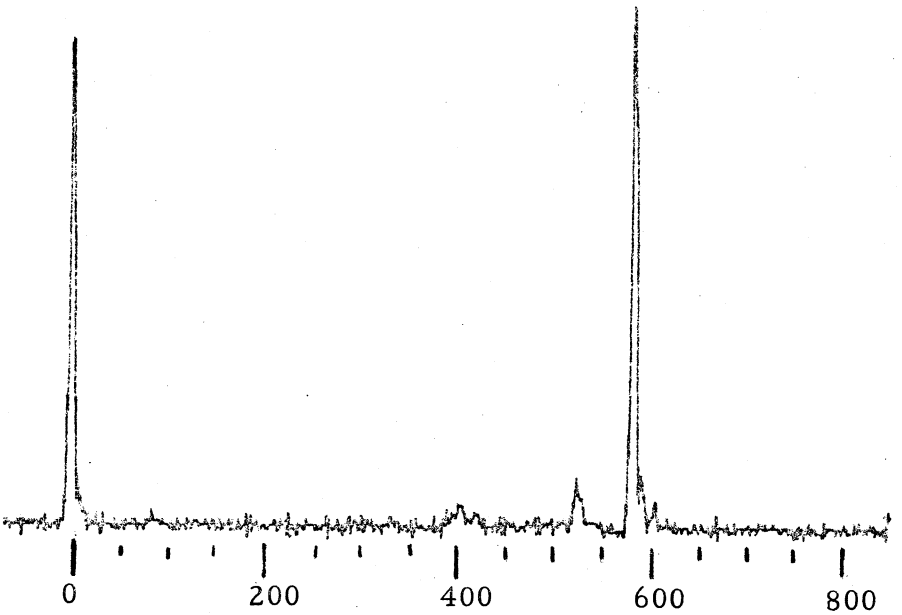

Time Delay - nanoseconds

(a) Power impulse response.

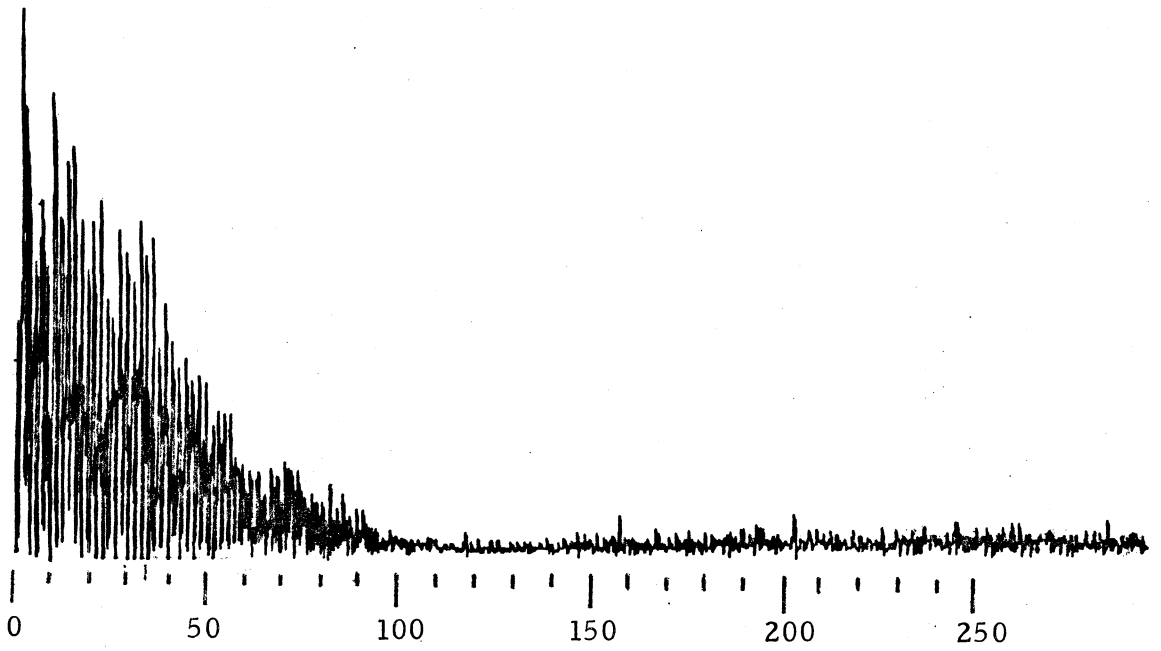

Frequency - MHz

(b) Frequency correlation function.

Figure 16. A response measured near the intersection of Baseline Road and 30th Street.

signal over the direct path was shadowed by buildings toward the west. A high-rise apartment building was located east of the van, and the impulse response of Figure 17(a) was measured. There is only a vestige of the direct path response and two delayed responses. The first is a strong reflection, at a delay of 230 ns, from the apartment building. The origin of the smaller reflection is not known, but it could be from another portion of the same building.

In an operational system, this type of response would generally mean that the direct path signal would be below the receiver threshold, and the recognized signal would be the large reflection. For a digital system the result could be a loss of synchronization. For example, seconds before this response was observed, the direct-path signal was strong with no reflections. As the van moved down the street, the direct signal was suddenly lost and the response of Figure 17(a) was measured. The sudden change in path length would cause the receiver to lose sync, and would require a finite time to acquire the delayed input signal. Information is lost during that period.

The transform of this response is shown in Figure 17(b). The rapid fluctuation is again due to the delay of the smaller reflection, and is on the order of 4 to 5 MHz. A slower variation in the peak values of the fast fluctuations is also seen, and is on the order of 7 MHz. This fluctuation is due to the differential delay between the two reflected components. Note also that there are two prominent lobes in the envelope of the correlation function, with a null at about 38 MHz. This characteristic is due to the delay-spread about the large reflection, and due to the delay of the component we can observe more than one cycle in the envelope.

5.3 Downtown Business Area

The central business district of Boulder is not typical of a large city. There are only a few buildings that are over three to four floors in height. In addition, the main business street

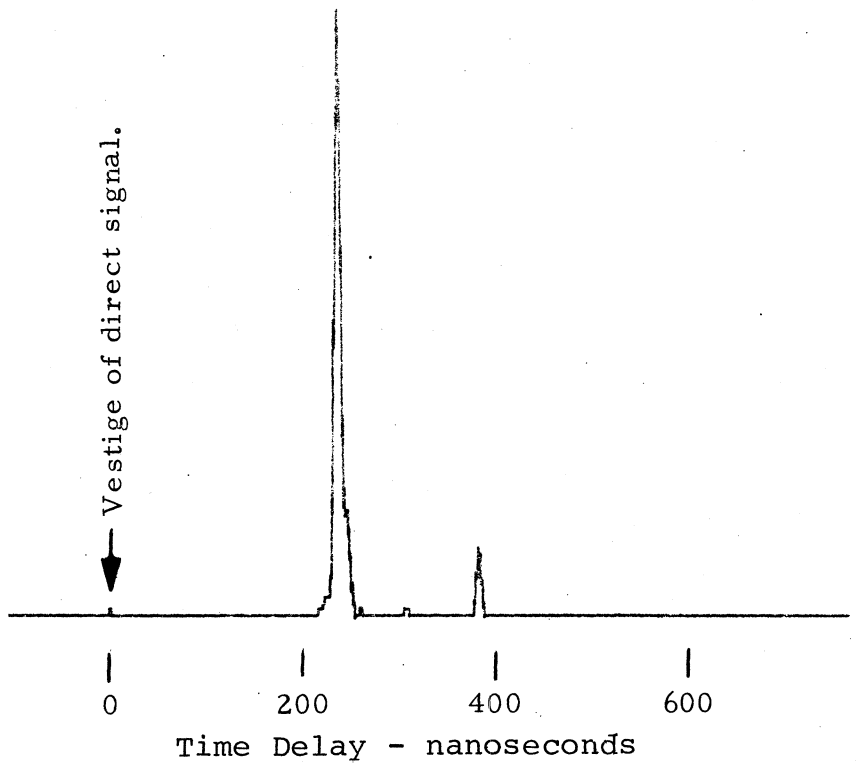

(a) The power impulse function.

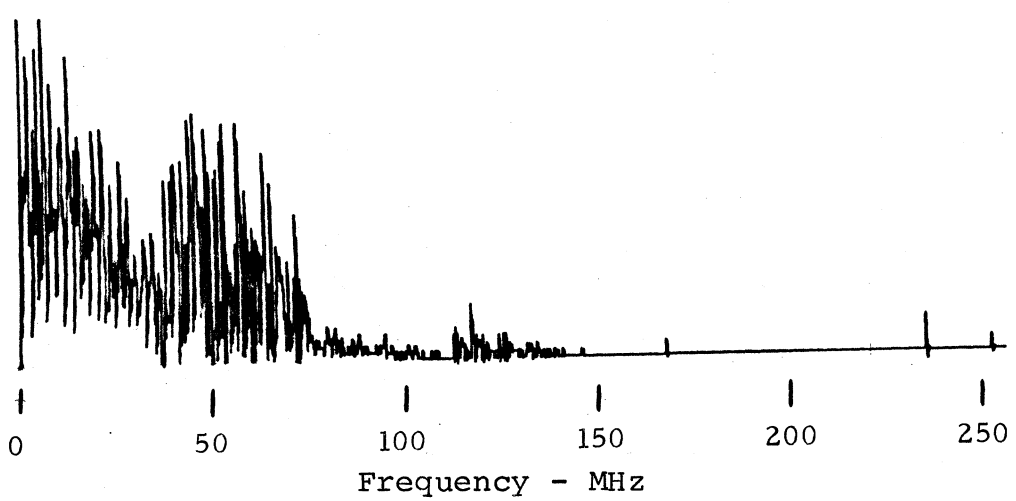

(b) The frequency correlation function.

Figure 17. A response where the direct signal is blocked by obstructions, showing reflections from an adjacent building.

is a pedestrian mall, and street traffic is routed in a counter-clockwise pattern around the five-block mall. Measurable multi-path in this vicinity was generally observed when the van was in an intersection of streets where a clear view toward the trans-mitter was provided. A typical response observed at the intersection of 15th and Walnut streets is shown in Figure 18(a). This intersection is at the SE corner of the traffic loop around the mall. Note that the response contains a direct-path signal and two delayed reflections (150 ns and 690 ns). The large reflection with the long delay-time is believed to be a reflec-tion from the Colorado Building at the corner of 14th and Walnut streets. This building is nine stories high, and is the tallest building in the downtown area. We were not able to stop the van in the intersection to verify the origin of the reflections.

The frequency correlation function of the response is shown in Figure 18(b), and an expanded scale plot is shown in Figure 18(c). The coherence BW is seen to be less than 1 MHz for this response, even though spectral energy is seen out to frequencies near 100 MHz. A cyclic variation on the order of 6 MHz can be observed in the expansion of the correlation function, corresponding to the delay of the first small reflection.

5.4 Major Arteries Through the City

One of the most interesting locations for reflections was observed along Broadway near the University of Colorado. The street is a major artery through Boulder (north/south), and the direct signal path between the probe transmitter and receiver van was clear. Near the intersection of Broadway and 13th streets, the response shown in Figure 19(a) was measured. A single reflection several dB larger in response than the direct path is seen at a delay of about 80 ns. The Fourier transform of the response is shown in (b) of the figure, where a cyclic response of 12.5 MHz is seen. Note also that the spectral energy has been limited to a value near 100 MHz, due to the time spread around both the direct and reflected signals. The

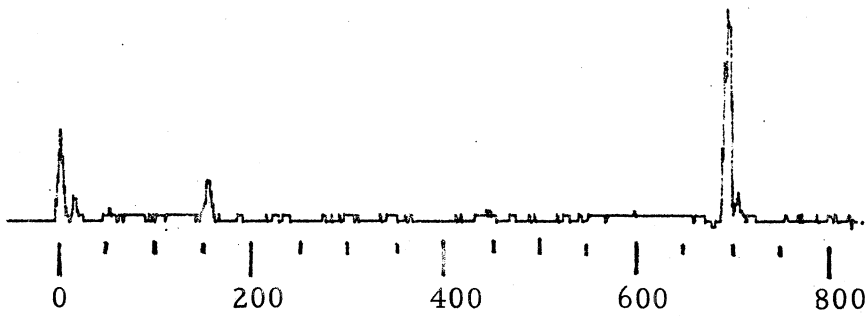

Time Delay - nanoseconds

(a) The power impulse function.

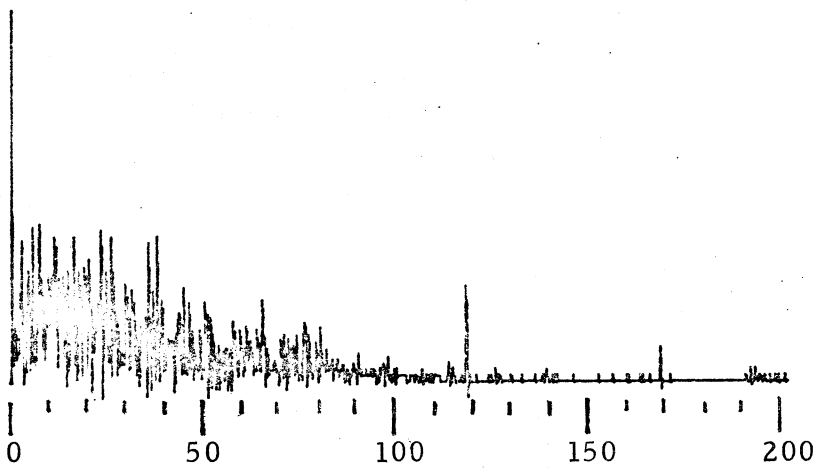

Frequency - MHz

(b) The frequency correlation function.

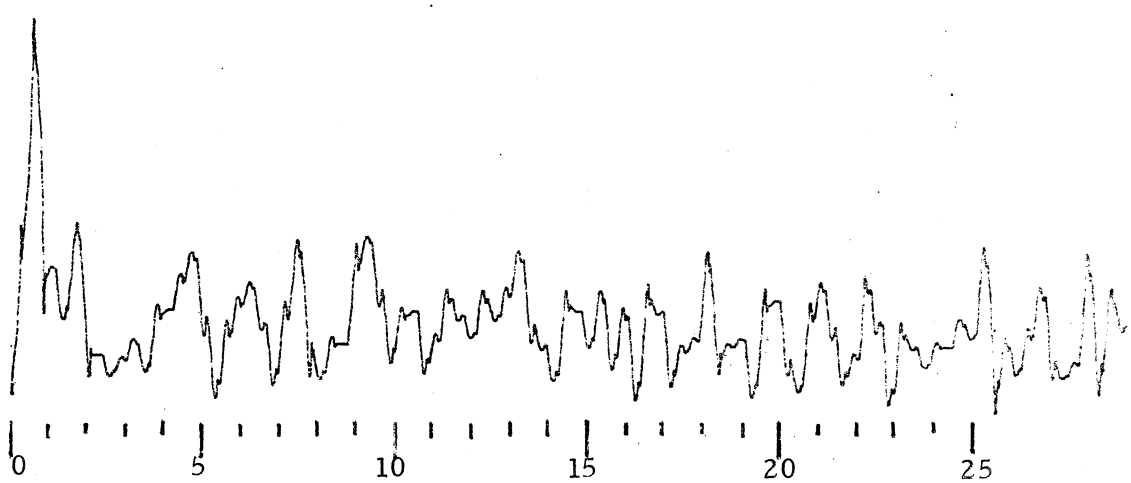

Frequency - MHz

(c) Expanded plot of (b).

Figure 18. A typical response measured in downtown Boulder, Colorado.

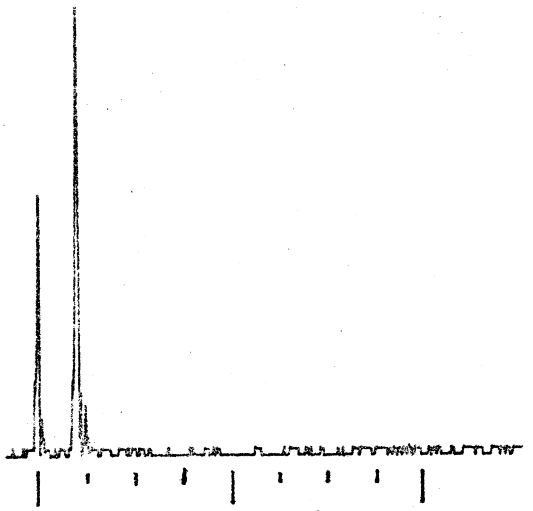

(a) The power impulse function.

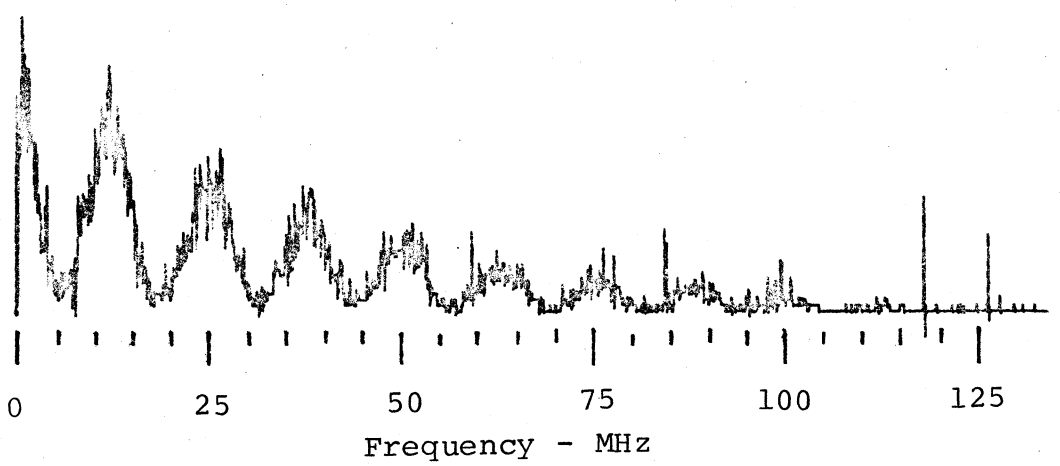

(b) The frequency correlation function.

Figure 19. A response measured near the intersection of Broadway and 13th Streets.

coherence bandwidth is seen to be on the order of 3 MHz in this instance.

As the receiver van proceded north along Broadway, the response changed to one of many reflected paths. An example is shown in Figure 20. The impulse response in (a) indicates several reflected signals spread in delay time over approximately 100 ns. An expanded scale of the response is shown in Figure 20(b), where at least seven individual reflected components can distinguished. Other examples were observed that displayed 10 or more reflections within this delay spread. The area is characterized by large university campus buildings east of the receiver van, and several large fraternity houses and university service buildings west of the van. This particular location provided the most complex multipath structure observed anywhere in the city.

Figure 21 presents the Fourier transform of the time function of Figure 20. The correlation function has a very sharp spike that is not discernable in Figure 21(a). The function is shown on an expanded scale in Figure 21(b), where the width of the correlation spike is seen to be less than 0.5 MHz, with a complete spectral null at that frequency. The spectral energy in Figure 21(a) is spread to about 80 MHz, but the coherence band is extremely narrow.

An average of the responses seen in this vicinity was analyzed from the magnetic tape recording. Figure 22 shows the delay spread of 100 individual impulse responses (10 responses/s) averaged in time over a period of 10 seconds. During this time the van moved approximately 15 ft (5 m) north along Broadway. A comparison of the averaged response with the individual response of Figure 20, indicates that only minor changes and time-delay shifts occurred during the interval. The expanded-scale plot of the delay-spread function in Figure 22(b) shows a number of distinct responses that obviously did not change a great deal in the 100-frame average. The total delay spread is just slightly over 200 ns, which is approximately the extent of the abcissa in Figure 22(b).

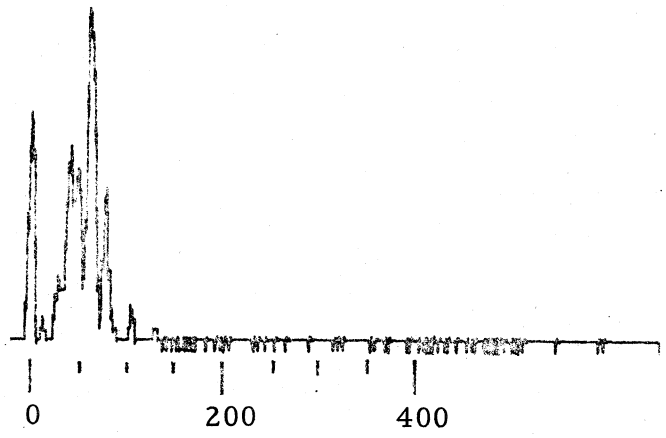

Time Delay - nanoseconds

(a) The power impulse function.

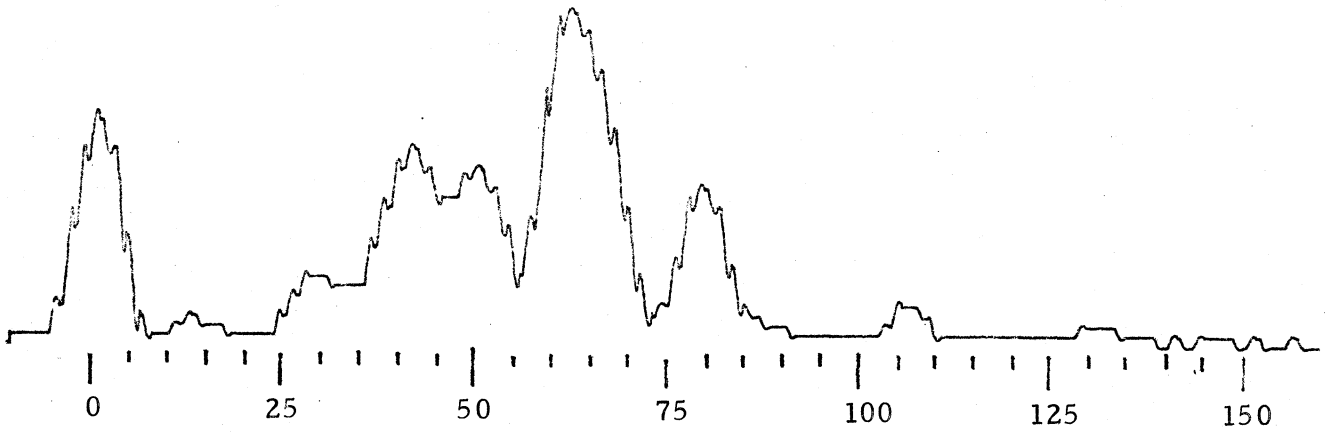

Time Delay - nanoseconds

(b) Expanded scale plot of (a).

Figure 20. Multipaths observed along Broadway near the University of Colorado.

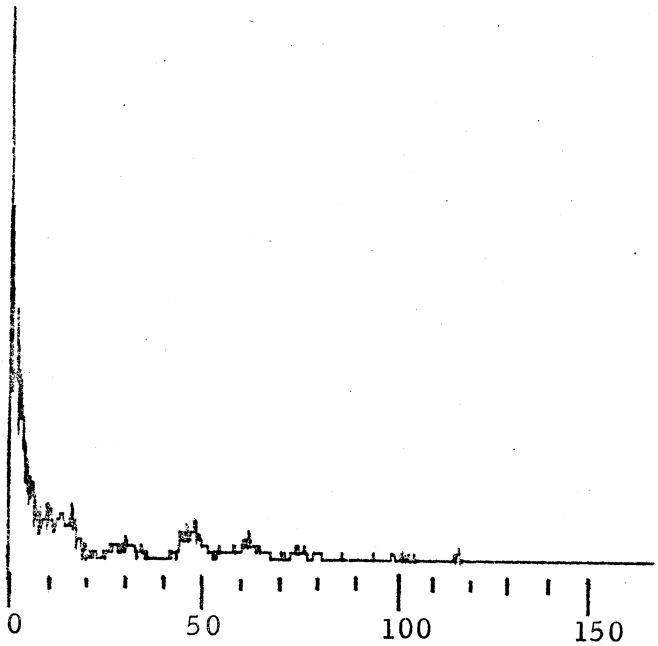

(a) The frequency correlation function.

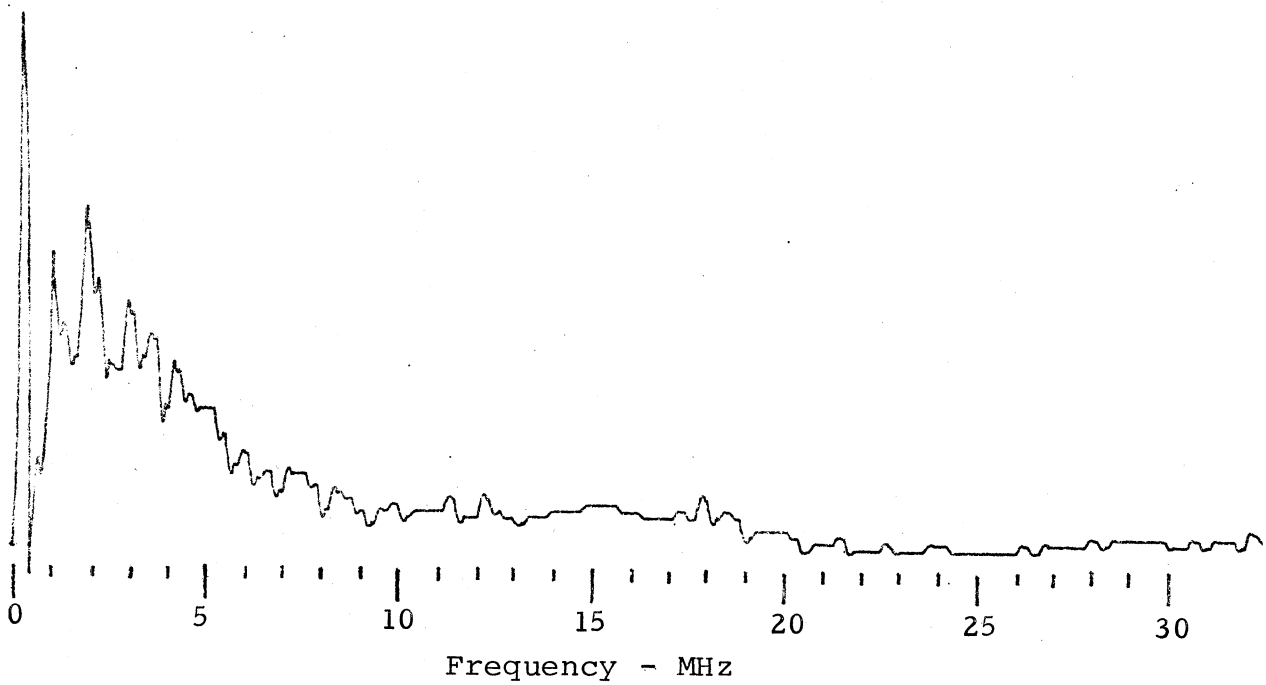

(b) Expanded scale plot of (a).

Figure 21. The Fourier transform (frequency correlation function) of the power impulse response of Figure 20.

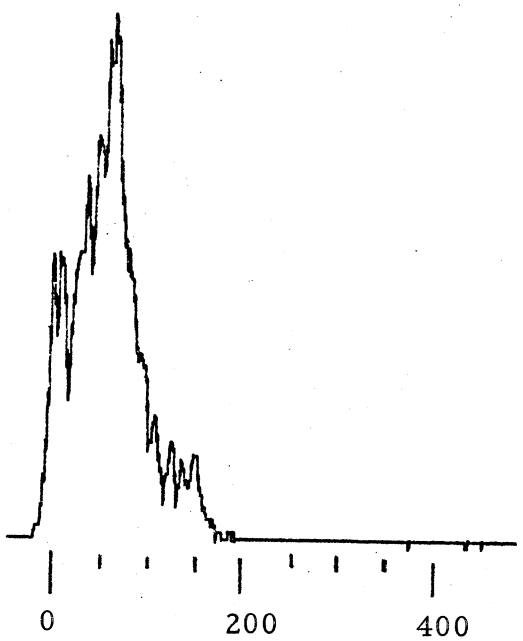

Time Delay - nanoseconds

(a) The averaged power impulse response.

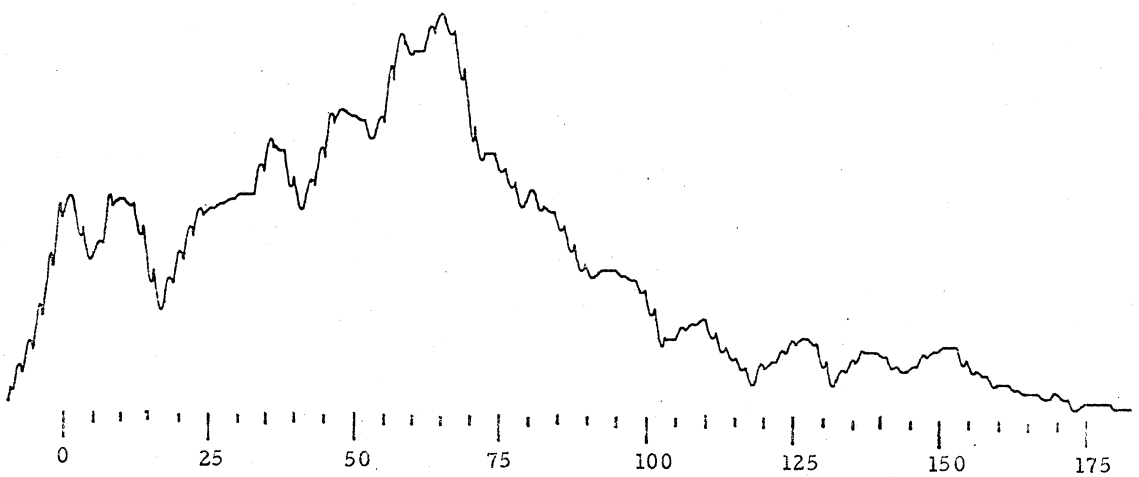

Time Delay - nanoseconds

(b) Expanded scale plot of (a).

Figure 22. An average of 100 impulse measurements recorded as the receiver van moved approximately 20 m along Broadway near College Avenue.

The frequency correlation function for the time-averaged response above is shown in Figure 23. Part (a) of the figure shows the complete spectral transform and part (b) is an expanded scale plot. The result is similar to that of the single response in Figure 21, however, a complete null in the correlation function at 0.5 MHz does not occur on the average. The average for the coherence bandwidth from Figure 23(b) is seen to be on the order of 2.5 to 3 MHz, and the total spectral energy is confined to approximately 10 MHz. The calibration function of Figure 12 is sketched in Figure 23(a) for a direct comparison of the channel response with the transmitted function. A spectral compression factor of approximately 10 to 15 is observed.

Another interesting example was measured along 28th St., which is U.S. Highway 36 through Boulder in a north-south direction. At a distance of approximately 4 km from the transmitter, the receiver van was adjacent the YMCA Building on North 28th Street. The direct-path signal was attenuated by other buildings and trees. The response shown in Figure 24 was measured as the van passed west of the YMCA, moving north along the street. Two reflections are seen at delays of about 30 and 55 ns. The first reflection is about 22 times the magnitude of the direct response, and the second smaller reflection about 9 times the direct magnitude. The frequency correlation function of this response is shown in Figure 25. The first significant feature to notice is the null in the response at the zero or reference frequency. This is due to the fact that only a vestige of the direct path response is seen in Figure 24. The fluctuation on the order of 15 MHz is due to the longest delayed signal. However, deep nulls are seen in the envelope of the function at roughly 15 MHz and 55 MHz. The spacings between these nulls correspond to the delay-time spacing between the two reflections, which is approximately 25 ns. The total spectral response has been limited to approximately 100 MHz. The spacing between spectral peaks ranges from about 12 MHz to 20 MHz, corresponding roughly to the delay-time of the second reflection.

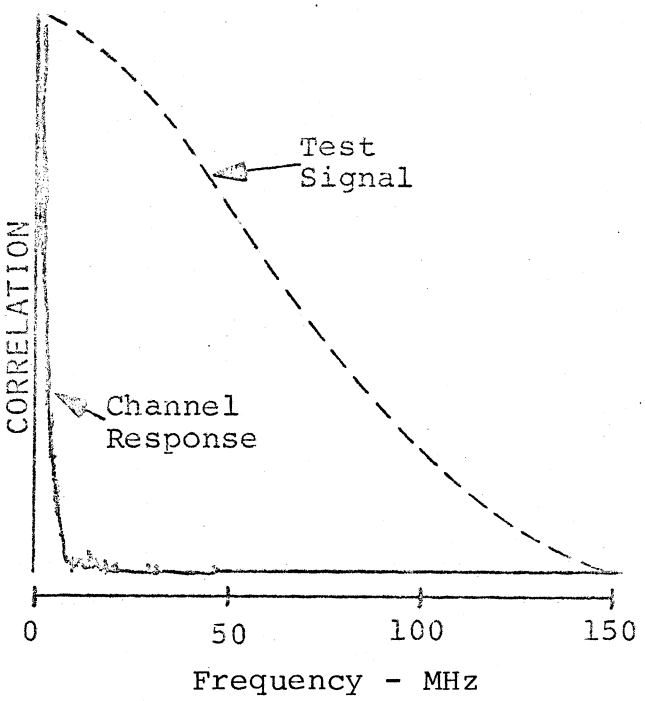

(a) The channel response compared with the test signal.

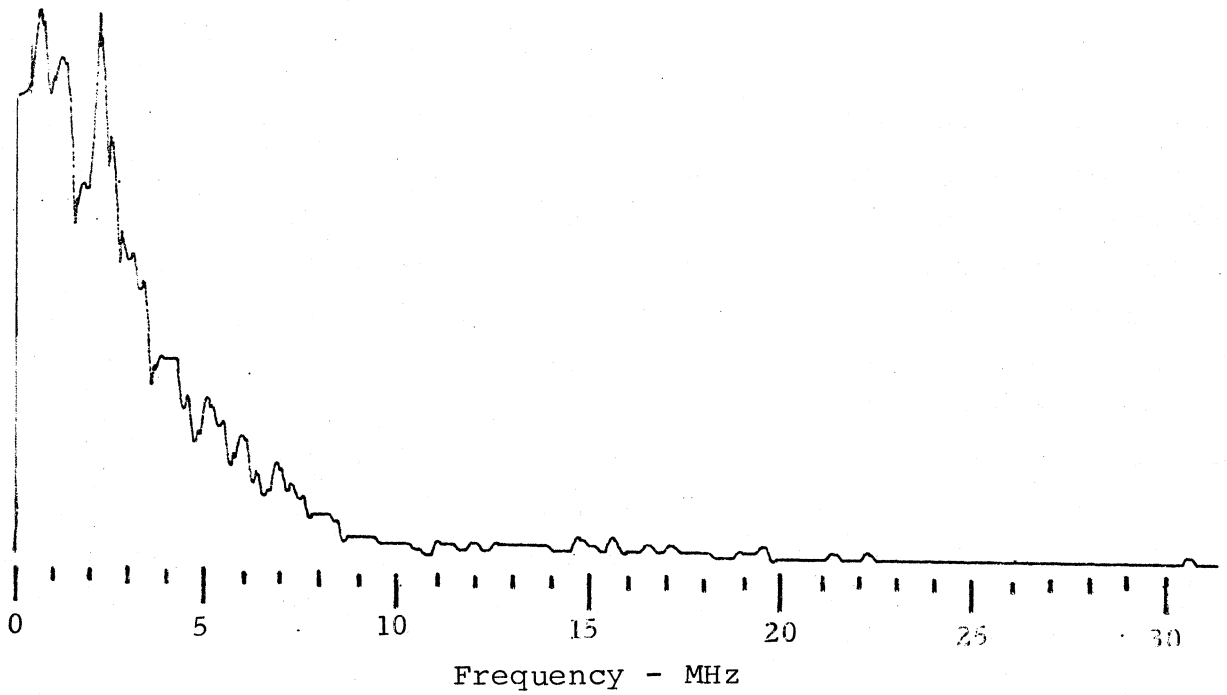

(b) Expanded scale plot of the channel response of (a).

Figure 23. The frequency correlation function of the time-averaged impulse response of Figure 22.

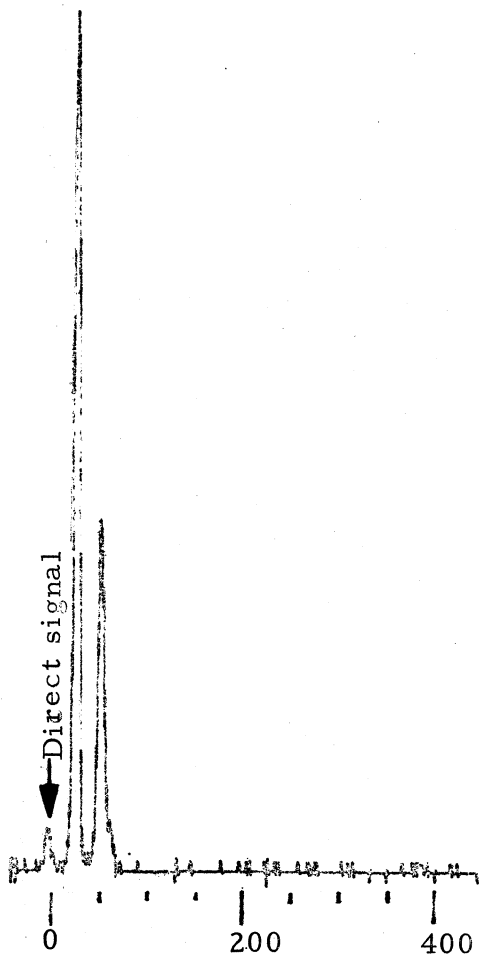

Figure 24. An impulse response measured on 28th Street, near the YMCA.

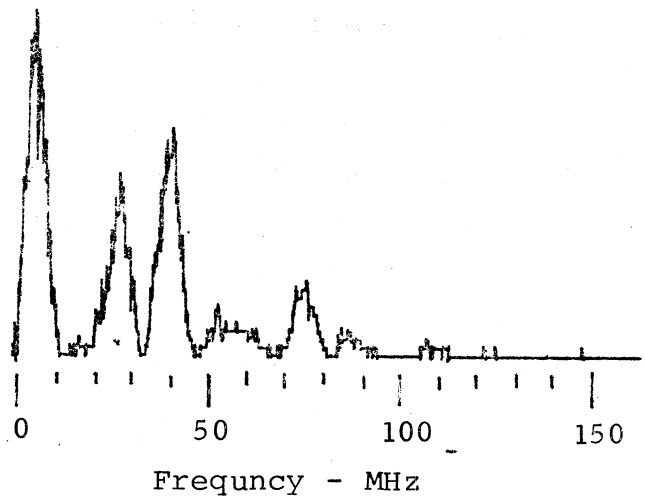

Figure 25. The frequency correlation function for the response shown in Figure 24.

5.5 Summary Remarks

The analyses presented in this section are only representative of the observed data, and the data-processing methods possible. It should be kept in mind that the data collection and format methods used in this project are ideal for obtaining information about the statistical variability of the mobile radio channel. Other correlation functions and the complete scattering function discussed in Section 4 can be derived in similar fashion from the magnetic tape data.

6. CONCLUSIONS AND RECOMMENDATIONS FOR FUTURE STUDIES

The effort reported here was conducted by the ITS Channel Characterization Group under a limited in-house support program. The primary objective was to demonstrate the existing capabilities for measuring and analyzing channel characteristics. Measurements of this type should be very beneficial to the designer of advanced communication systems. It is also important to measure performance of high-data rate systems over transmission channels with known characteristics so that the channel's impact on capacity and performance (in terms of data rate and error rate) can be determined.

The signaling and data rates for various links and channel responses have usually been deduced theoretically based on certain assumptions and a limited amount of data (Linfield, 1977). One's confidence in these estimates would be greatly enhanced if comparisons could be made with actual performance data. Unfortunately, such data are severely lacking. Several workers have measured responses on radio channels, and others have measured system performance including error rates on channels. Seldom, however, have the two been measured simultaneously (and at rates where selective fading occurs) in spite of the fact that both measurement techniques are well established.

In the future, one might expect a greater channelization of spectrum bandwidth as filter technology advances. This, coupled with the increasing demand for higher data rates, implies a need

for signal designs and modulation techniques that will maximize the number of bits that can be transmitted on a per-unit-of-bandwidth basis.

Designers of systems will need a comprehensive data base covering the higher frequency bands to characterize the transmission channel and its effect on various signals. As time goes on, it becomes more and more difficult to obtain this data base because it requires broadband measurements over clear channels. Already portions of the spectrum are overcrowded, making it difficult to perform broadband impulse measurements and wideband performance measurements without encountering interference from other users. This is particularly true in the land-mobile area where the lower bands are already crowded with users in every city. Nielson (1975), for example, was unable to measure the impulse response in the 400 MHz land mobile band because of the intense interference which existed in the San Francisco Bay Area.

Because a firm data base is so essential to the design of systems that are to make maximum use of the limited spectrum, it is recommended that measurement programs be instituted to characterize various radio transmission channels (where they are still clear) as soon as possible. These programs should include both additive noise and response data (either in the frequency domain or the time domain) over a variety of links and transmission channels with emphasis in the SHF band (3-30 GHz). Impulse response measurements should use the highest practical resolution; i.e., over bandwidths on the order of 10% of the carrier frequency.

Continuous recordings of the response and the noise should, after processing, be capable of providing an appropriate measure of the time and frequency dispersiveness of the channel and a statistical representation of the noise. At the same time, the error performance of a system should be measured at various data rates, using a convenient modulation scheme such as quadrature PSK so that performance predictions can be verified.

All too often the additive noise has been assumed to be white with a constant noise power spectral density. This, of

course, is not always the case and particularly not for the mobile environment. Here the primary error-causing additive noise is more likely to be man-made, either ignition or power-line noise with impulsive properties, or interference from adjacent channels. Measurement programs which are designed to characterize the channel should include additive-noise measurements commensurate with the response and performance measurements, and an attempt should be made to resolve the error-causing effects.

An accurate wideband characterization of the multiplicative and additive noise in the radio channel is essential to the future development of advanced communication systems. Statistical models based on experimental data are also useful for simulation experiments in order to avoid costly hardware tests of ad hoc systems. An example of this latter application is given by Suzuki (1977), who utilized some experimental data obtained by Turin et al. (1972) to establish a statistical model for the urban radio propagation medium.

7. ACKNOWLEDGEMENTS

The authors wish to acknowledge the contributions of L.E. Pratt and C.M. Minister to this program. Mr. Pratt was responsible for the design and fabrication of the high-resolution probe used in the measurements. He also prepared and tested the apparatus for the experiments, installed the equipment, and operated the receiver van with the able assistance of Mr. Minister.

8. REFERENCES

Bello, P.A., J.K. DeRosa, and C.J. Boardman (1973), Line-of-sight wideband propagation, Final Technical Report RADC-TR-73-167, Rome Air Development Center, Griffiss AFB, NY, May.

Bussgang, J.L., E.H. Getchell, G. Goldberg and P.F. Mahoney (1976), Stored channel simulation of tactical VHF radio links, IEEE Trans. Comm. Tech., COM-24, No. 2, 154-163.

Cox, D.C. (1972a), Delay doppler characteristics of multipath propagation in a suburban mobile radio environnment, IEEE Trans. Ant. and Prop., AP-20, No. 5, 625-635.

Cox, D.C. (1972b), Time- and frequence-domain characterizations of multipath propagation at 910 MHz in a suburban mobile-radio enviornment, Radio Science, Vol. 7, No. 12, 1069-1077.

Gallager, R.G. (1964), Characterization and measurement of time and frequency-spread channels, Tech. Report No. 352, Mass. Inst. of Tech., Lincoln Laboratory, Lexington, MA.

Hubbard, R.W. (1971), Characterization of multiplicative noise in propagating systems, IEEE Electromagnetic Compatability Conference Record, Tuscon, AZ, November.

Kailath, T. (1959), Sampling models for a linear time-variant filter, MIT Research Lab. of Electronics, Report No. 352, May.

Linfield, R.F. (1977), Radio channel capacity limitations, Office of Telecommunications, OT Report 77-132, November.

Linfield, R.F., R.W. Hubbard, and L.E. Pratt (1976), Transmission channel characterization by impulse response measurements, Office of Telecommunications, OT Report 76-96, August.

Nielson, D.L. (1975), Microwave propagation and noise measurements for mobile digital radio applications, Packet Radio Note 4, Contract DAHC15-73-C-0187, Stanford Research Institute, Menlo Park, CA, January.

Suzuki, H. (1977), A statistical model for urban radio propagation, IEEE Trans. on Comm., COM-25, No. 7, 673-680.

Turin, G.L., F.D. Clapp, T.L. Johnston, S.B. Fine, and D. Larry (1972), A statistical model of urban multipath propagation, IEEE Trans. on Vehic. Tech., VT-20, No. 1, 1-9.

FORM OT-29
(3-73)

U.S. DEPARTMENT OF COMMERCE
OFFICE OF TELECOMMUNICATIONS

BIBLIOGRAPHIC DATA SHEET

	1. PUBLICATION OR REPORT NO. NTIA-Report-78-5	2. Gov't Accession No.
3. Recipient's Accession No.		
4. TITLE AND SUBTITLE MEASURING CHARACTERISTICS OF MICROWAVE MOBILE CHANNELS		5. Publication Date June 1978
		6. Performing Organization Code NTIA/ITS
7. AUTHOR(S) R.W. Hubbard, R.F. Linfield, and W.J. Hartman		9. Project/Task/Work Unit No. 9101900
8. PERFORMING ORGANIZATION NAME AND ADDRESS Institute for Telecommunication Sciences National Telecommunications and Information Administration U.S. Department of Commerce, Boulder, CO 80302		10. Contract/Grant No.
11. Sponsoring Organization Name and Address Institute for Telecommunication Sciences National Telecommunications and Information Administration U.S. Department of Commerce, Boulder, CO 80302		12. Type of Report and Period Covered NTIA Report, FY 77
		13.

14. SUPPLEMENTARY NOTES

15. ABSTRACT *(A 200-word or less factual summary of most significant information. If document includes a significant bibliography or literature survey, mention it here.)*

This report describes the application of a high resolution (6 ns) pseudo-random noise (PN) channel probe for evaluating the transmission character of a land-mobile communication channel. Preliminary measurements were performed at a microwave frequency in a number of locations in Boulder, Colorado. Examples of data are presented which characterize the frequency correlation of the channel transfer function, and provide additional information on the spectral distortions caused by multipath.

The data processing and analysis techniques are emphasized in the report, as they are ideally suited to developing a useful statistical summary of channel parameters. The methods are rapid, and are made from data recorded in standard analog magnetic tape in the field locations. It is recommended that a wideband channel characterization program ve undertaken in the near future before spectrum congestion precludes obtaining useful data.

16. Key Words ~~(Alphabetical order, separated by semicolons)~~

Channel characterization; frequency correlation function; impulse response; land-mobile radio; microwaves, multipath

17. AVAILABILITY STATEMENT [X] UNLIMITED. [ ] FOR OFFICIAL DISTRIBUTION.	18. Security Class *(This report)* Unclassified	20. Number of pages 53
	19. Security Class *(This page)* Unclassified	21. Price:

★U.S. Government Printing Office: 1978-778-103/361 Region 8

USCOMM-DC 29716-P73